



HAL
open science

Staging and normal table of postembryonic development of the clownfish (*Amphiprion ocellaris*)

Natacha Roux, Pauline Salis, Anne Lambert, Valentin Logeux, Olivier Soulat,
Pascal Romans, Bruno Frédérich, David Lecchini, Vincent Laudet

► To cite this version:

Natacha Roux, Pauline Salis, Anne Lambert, Valentin Logeux, Olivier Soulat, et al.. Staging and normal table of postembryonic development of the clownfish (*Amphiprion ocellaris*). *Developmental Dynamics*, 2019, 248 (7), pp.545-568. 10.1002/dvdy.46 . hal-02272895

HAL Id: hal-02272895



<https://hal.sorbonne-universite.fr/hal-02272895v1>

Submitted on 28 Aug 2019

HAL is a multi-disciplinary open access archive for the deposit and dissemination of scientific research documents, whether they are published or not. The documents may come from teaching and research institutions in France or abroad, or from public or private research centers.

L'archive ouverte pluridisciplinaire **HAL**, est destinée au dépôt et à la diffusion de documents scientifiques de niveau recherche, publiés ou non, émanant des établissements d'enseignement et de recherche français ou étrangers, des laboratoires publics ou privés.

Staging and normal table of postembryonic development of the clownfish (*Amphiprion ocellaris*)

Natacha Roux^{1,2}  | Pauline Salis¹ | Anne Lambert³ | Valentin Logeux¹ | Olivier Soulat⁴ | Pascal Romans¹ | Bruno Frédéricich⁵ | David Lecchini^{2,6} | Vincent Laudet¹ 

¹Observatoire Océanologique de Banyuls-sur-Mer, CNRS UMR 7232 BIOM, Sorbonne Université, Banyuls-sur-Mer, France

²PSL Research University, USR 3278, EPHE-CNRS-UPVD, Moorea, French Polynesia

³Institut de Génomique Fonctionnelle de Lyon, Université Claude Bernard Lyon, Ecole Normale Supérieure de Lyon, Lyon, France

⁴Aquarium de Canet-en-Roussillon, Canet-en-Roussillon, France

⁵Laboratory of Functional and Evolutionary Morphology, FOCUS, University of Liège, Liège, Belgium

⁶Laboratoire d'Excellence CORAIL, Moorea, French Polynesia

Correspondence

Vincent Laudet, Observatoire Océanologique de Banyuls-sur-Mer, CNRS UMR 7232 BIOM, Sorbonne Université, 1 Avenue Pierre Fabre, 66650 Banyuls-sur-Mer, France.
Email: vincent.laudet@obs-banyuls.fr

Funding information

Contrat de Projet Etat-Polynésie française 2015-2020, LabEx Corail, Grant/Award Number: project Etape, PSL environment - project Pestico; Centre National de la Recherche Scientifique; Agence de l'eau; Rhone Méditerranée Corse - n° 2018 1765

Abstract

Background: The clownfish *Amphiprion ocellaris* is one of the rare coral reef fish species that can be reared in aquaria. With relatively short embryonic and larval development, it could be used as a model species to study the impact of global changes such as temperature rise or anthropogenic threats (eg, pollution) on the postembryonic development at molecular and endocrinological levels. Establishing a developmental table allows us to standardize sampling for the scientific community willing to conduct experiments on this species on different areas: ecology, evolution, and developmental biology.

Results: Here, we describe the postembryonic developmental stages for the clownfish *A. ocellaris* from hatching to juvenile stages (30 days posthatching). We quantitatively followed the postembryonic growth and described qualitative traits: head, paired and unpaired fins, notochord flexion, and pigmentation changes. The occurrence of these changes over time allowed us to define seven stages, for which we provide precise descriptions.

Conclusions: Our work gives an easy system to determine *A. ocellaris* postembryonic stages allowing, thus, to develop this species as a model species for coral reef fishes. In light of global warming, the access to the full postembryonic development stages of coral reef fish is important to determine stressors that can affect such processes.

KEYWORDS

coral reef fish, developmental stages, ontogeny, pigmentation, Pomacentridae, postembryonic

1 | INTRODUCTION

Coral reefs occupy 2 284 300 km², representing only 0.09% of ocean surface.¹ Although rare, reefs are nonetheless one of the

most diverse marine ecosystems, inhabited by 800 hard coral species and more than 4000 species of fish.^{2,3} Coral reefs are economically important, providing ecosystemic services such as tourism, fishing, coastal protection, pharmaceutical chemicals,

This is an open access article under the terms of the Creative Commons Attribution-NonCommercial License, which permits use, distribution and reproduction in any medium, provided the original work is properly cited and is not used for commercial purposes.

© 2019 The Authors. *Developmental Dynamics* published by Wiley Periodicals, Inc. on behalf of American Association of Anatomists.

and natural products.⁴ More than 500 million people rely on these ecosystems for food, coastal protection, and economic resources. According to Cesar et al.,⁵ coral reefs provide \$30 billion/year to the global economy. Despite the major importance of these ecosystems, no coral reef fish are currently used as a biological model organism such as mice, Zebrafish, or drosophila.

Most coral reef fishes have a biphasic life history, with an oceanic larval phase lasting from one to six weeks (depending on the species) as well as a reef benthic phase for juveniles and adults.⁶ The oceanic phase is critically important as it allows population connectivity, maintenance of high genetic diversity, and replenishment of adult populations.⁷ The transition between the oceanic and the benthic phases, called recruitment, entails morphological, physiological, and behavioral changes that correspond to a metamorphosis triggered, in most studied species, by thyroid hormones.⁸ The recruitment phase ends when larvae enter the reef, passing from a pelagic to a benthic/demersal lifestyle. This transition is critical in adapting individuals for life in a reef habitat, allowing crucial maturation processes such as the acquisition of sensory abilities to locate reef and suitable microhabitat.^{9,10}

Metamorphosis is defined as a critical postembryonic developmental transformation that is crucial for the maintenance of adult reef fish populations and particularly sensitive to the anthropogenic stressors affecting coral reefs.^{11,12} We recently demonstrated that environmental pollutants, such as chlorpyrifos, severely impair the larval transformation and sensory abilities of the convict surgeonfish *Acanthurus triostegus* and that exposure to these pollutants result in juveniles of poor quality.^{8,13} Other pollutants, such as polycyclic aromatic hydrocarbons (PAH) (components of petroleum), are also known to affect growth rates, habitat settlement, and antipredator behaviors of larval coral reef fishes.¹⁴ Coral reef fish larvae are also exposed to many other threats, including ocean acidification,^{15,16} sediment pollution,¹⁷ anthropogenic noise,¹⁸ and sea temperature rise.¹⁹ All these stressors are known to disrupt sensory development and antipredatory behaviors and likely decrease individual survival rates.^{10,16} Because reef fish larvae often undergo extensive oceanic dispersal and may be difficult to rear in culture, normal developmental processes of these species are often poorly described. In order to better understand how anthropogenic stressors affect biological processes such as larval development and metamorphosis, it is essential to thoroughly describe and functionally analyze the processes of normal larval and juvenile development. Indeed, a well defined and complete developmental series is essential for thorough study of any species, but this has not yet been produced for any coral reef fish.

The false clownfish *Amphiprion ocellaris* (Cuvier 1830) is the most widely used coral reef fish in a laboratory setting, as it is relatively easy to rear in aquaria.²⁰⁻²⁴ Living in symbiosis with sea anemones (*Stichodactyla gigantea*, *S. mertensii*, *Heteractis magnifica*), this clownfish is native to the Indo-West Pacific region from Indo-Malayan Archipelago to the Philippines and

northwestern Australia. *A. ocellaris* has been used as a model for ecological studies; groups have assessed the sensory abilities of reef fish larvae and the impact of environmental perturbations on habitat and predation detection.^{16,24,25} Its embryonic development has been precisely described,²⁶⁻²⁸ and classical techniques of developmental biology, including in situ hybridization, have been successfully performed on clownfish embryos.^{29,30}

A. ocellaris belongs to the Pomacentridae family, which comprises 30 species (29 *Amphiprion* and 1 *Premnas*)^{31,32} and more than 300 species of damselfish.³³ This family is thus one of the dominant actinopterygian fish groups on coral reefs. Its phylogenetic position (exemplified by *A. ocellaris* and the damselfish *Stegastes partitus*, whose genomes have been sequenced) is shown in Figure 1. It illustrates how it is nested in the late radiation of the Perciformes, cichlids being the closest classical fish model.³⁴⁻³⁶ Pomacentrids have developed fascinating innovations that can provide fertile ground for evo-devo studies. For example, they independently evolved jaw protrusion ability, thus providing one case of this convergent feature, allowing the analyses of how different ontogenetic

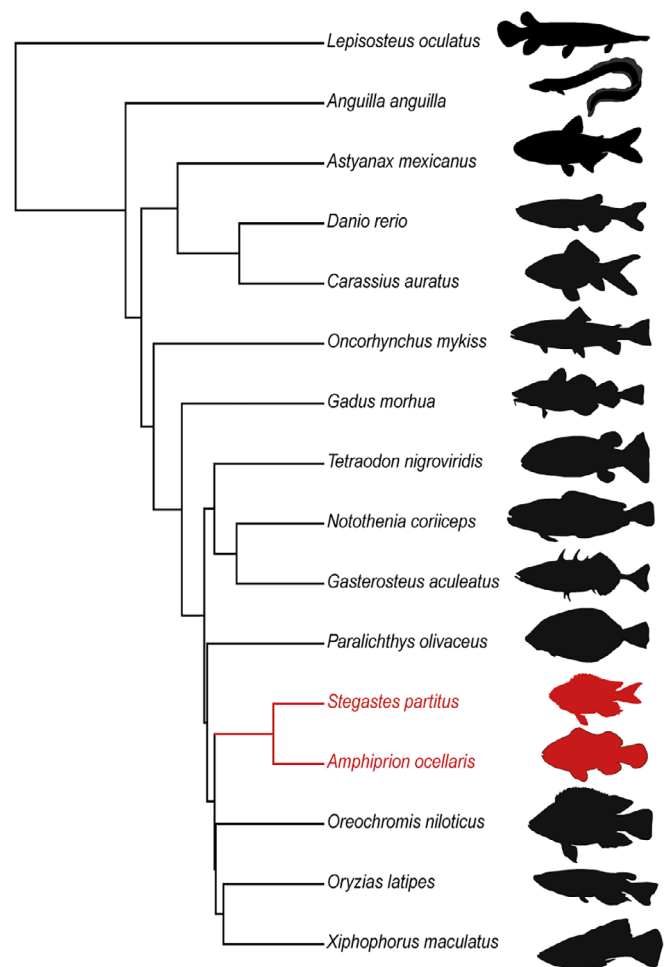


FIGURE 1 Phylogeny of 16 representative fish species used in developmental biology or evolutionary sciences, including the clownfish *c* and the damselfish *Stegastes partitus* (both colored in red)

trajectories reach similar solutions.³⁷ In addition, they possess peculiar anatomical traits to graze filamentous algae and to produce sounds during numerous social interactions.³⁸⁻⁴⁰ The clownfish also provide a unique model for the evolution of pigment pattern that allows the study of how ecology and development can permit and constrain the diversification of complex patterns.^{30,41,42} Last, clownfishes developed unique symbiotic relationships with giant sea anemones. The recruitment of the young juveniles in their host, the development of the mechanisms preventing the stinging of the sea anemone nematocysts, the variable host specificity displayed by the different species, and the mechanisms by which several clownfish can share the same host are all basic biological issues that can be studied using this model and that can impact more broadly other kinds of symbiotic relationships between eukaryotic organisms.⁴³ Thus, clownfish is a new model species with a high potential to further study evolutionary and developmental processes in a unique ecological framework. However, to date, only few data are available on its postembryonic development.^{27,42,43} Establishing a developmental table for this species would be of particular interest to conduct evo-devo studies such as those listed above.

Developmental staging tables are essential systems for model organisms, as they allow assigning individuals to distinct developmental stages.⁴⁴ Staging tables are valuable and widespread tools for standardizing development, and embryonic staging tables are available for model organisms including the Zebrafish *Danio rerio*^{45,46} and the African clawed frog *Xenopus laevis*.⁴⁷ Stage identification and standardization are particularly important, since heterogeneity between individuals means that time alone is a limited measure of developmental state.^{48,49} Larval development depends on both genetic and

environmental factors such as temperature, photoperiod, food availability, and fish density.^{19,46,50-52} Establishing a developmental table for *A. ocellaris* will allow standardized sampling by the scientific community and will advance research using this species.

Our goals in this article are 3 fold: First, we describe the development of quantitative traits in postembryonic clownfish. Second, we describe the morphological changes occurring during the larval development of *A. ocellaris*, focusing on qualitative traits (fin development, notochord flexion, and pigmentation). Finally, we identify developmental stages that comprise a straightforward and useful system for standardizing larval stage.

2 | LIFE HISTORY STAGE DEFINITIONS

As do most of the coral reef fish, *A. ocellaris* have a biphasic life cycle with a dispersive oceanic phase and a more sedentary reef phase (Figure 2).

2.1 | Embryonic phase

In contrast to many coral reef fishes that spawn in the open ocean, clownfishes are benthic spawners. They lay their eggs attached to a rock in the immediate proximity of sea anemones.⁶ The embryonic phase occurs directly after fertilization and lasts until larvae are able to feed on exogenous food²⁷; this takes six to eight days in clownfishes, depending on temperature. This is longer than the embryonic phase in other species, including Zebrafish (48 hours) and sea bass (four days).^{45,53,54}

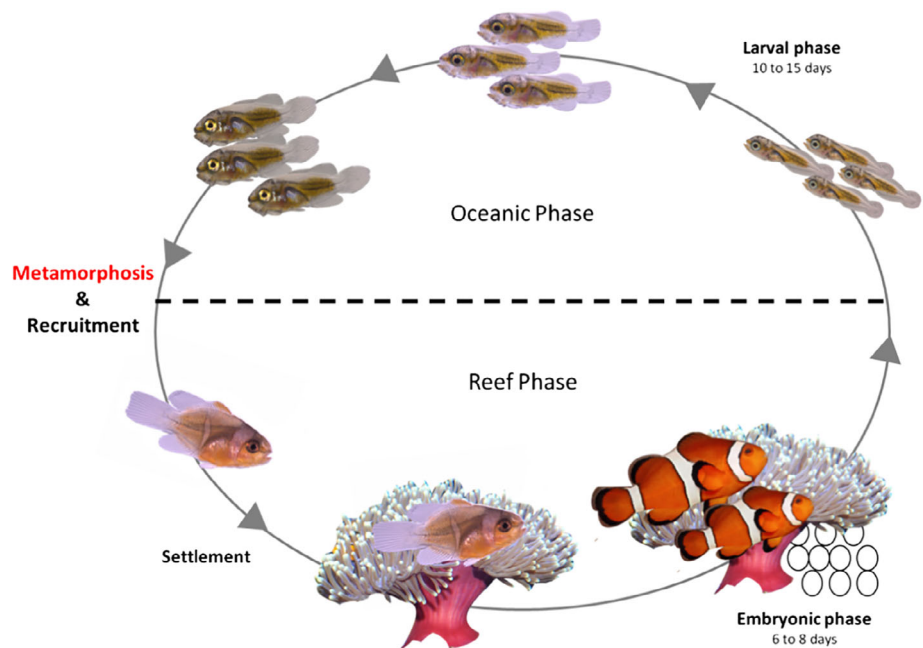


FIGURE 2 Life cycle of clownfish. Clownfishes lay their eggs close to their sea anemone, where they will develop between six and eight days depending on temperature. After hatching, larvae are directly dispersed into the open ocean, where they will grow between 10 to 15 days before returning to a reef. The transition between the ocean and the reef is associated with the metamorphosis of larvae into juveniles. Juveniles will then settle in a sea anemone

2.2 | Larval phase

This phase begins when newly hatched larvae are able to feed on exogenous food and, like in most marine teleosts, it corresponds to the oceanic dispersal phase.⁶ During this period, larvae undergo major morphological and physiological changes (fin differentiation, notochord flexion, sensory organs differentiation, organ differentiation)^{11,55}. This phase ends during a specific postembryonic step called metamorphosis, which introduces the transition between larva and juvenile.^{11,56,57} Clownfish species exhibit a short larval phase, lasting only 10 to 15 days compared to other larvae of coral reef fish species, which can spend 19 to 70 days in the ocean.^{53,58}

2.3 | Metamorphosis

In the context of this study, we define metamorphosis as a post-embryonic developmental step triggered by thyroid hormones and characterized by ecological, behavioral, morphological, and physiological changes. For the clownfish *A. ocellaris*, metamorphosis involves acquisition of three white stripes and corresponds to the transition of the juvenile phase.⁴² Indeed, when the white stripes appear on the head and body of *A. ocellaris*, a change of swimming behavior is observed in the tank: Larvae swim in the water column, while metamorphic and post-metamorphic fish swim closer to substrates. In the wild, this phase ends when young juveniles settle into a host sea anemone.

2.4 | Recruitment and settlement phases

In general, coral reef fishes, including *A. ocellaris*, have a clear ecological transition between the larval and the

juvenile phases, and these phases coincide with the oceanic and reef phases, respectively. This transition is called recruitment in ecology and is associated with the metamorphosis of larvae in juveniles. After metamorphosis, juveniles are ready to find a suitable habitat in a reef to pursue their growth and reach adult stage; this is the settlement phase^{10,59}

(Figure 2). Disruption of postembryonic development and metamorphosis may prevent successful recruitment and the settlement phases by increasing mortality of new recruits.

2.5 | Juvenile phase

As juveniles, individuals are ready to settle on suitable habitats (eg, sea anemone hosts for clownfish), where they continue to grow and mature.^{21,60} Juveniles possess most characteristics of adults but have not yet achieved reproductive maturity. Gametes mature in clownfish species only when an individual reaches the top of its social hierarchy in a sea anemone.^{61,62}

3 | RESULTS

3.1 | Developmental rate

The quantitative traits described in Table 1 were measured every day from 1 to 21 days posthatching (dph), and in juveniles at 30 dph. During growth, *A. ocellaris* undergoes two distinct developmental phases, one from 1 to 7 dph, and another from 8 to 21 dph. Growth rates are higher during the second phase (0.06 mm/day for the first phase, and 0.2 mm/day

TABLE 1 List of quantitative and qualitative traits used to describe clownfish postembryonic development

| | Quantitative trait | Trait description |
|---------------------|-------------------------|---|
| Quantitative traits | Standard length (SL) | Distance from the snout to the extremity of the notochord in preflexion larvae, and distance from the snout to the middle of the caudal peduncle in post flexion larvae |
| | Snout anus length (SAL) | Distance from the snout to the anus |
| | Head length (HL) | Distance from the snout to the extremity of the branchial opercular |
| | Body depth (BD) | Distance perpendicular to HL directly from the top of the head at the basis of the dorsal fin to the bottom of the body at the implantation of the pelvic fin |
| | Eye diameter (ED) | Distance at the longest axis of the eye |
| | Snout length (SL) | Distance from the snout to the first border of the eye |
| | Head Depth (HD) | Distance perpendicular to HL from the anus to the basis of the dorsal fin soft rays. |
| | Qualitative traits | Anal soft rays |
| Anal spines | | Appearance of the spines |
| Dorsal soft rays | | Appearance of the soft rays |
| Dorsal spines | | Appearance of the spines |
| Pelvic fin | | Development of the pelvic fin |
| White stripes | | Appearance of the three body white stripes |
| Notochord flexion | | Flexion steps of the notochord |

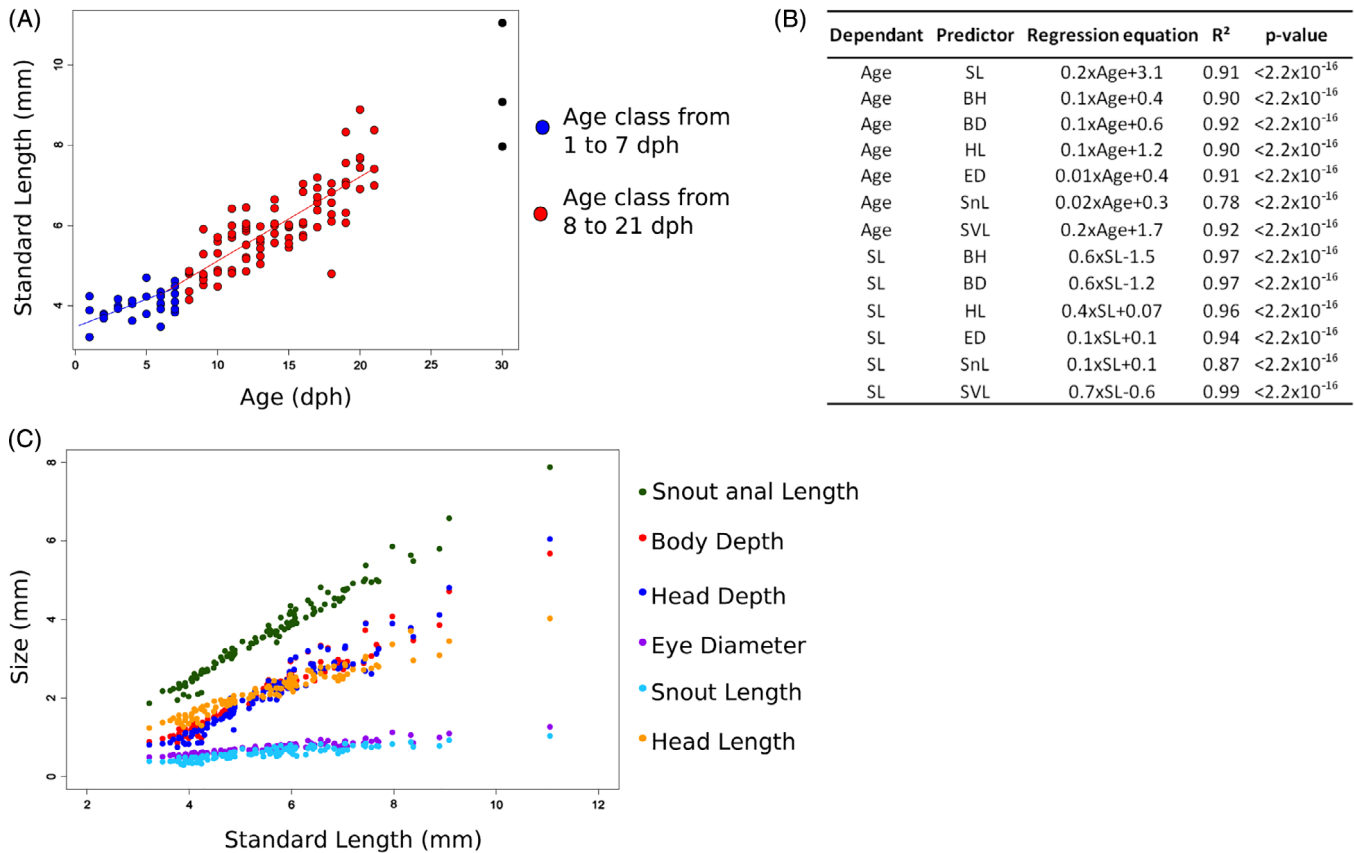


FIGURE 3 Development rates during *Amphiprion ocellaris* development. A: Graph showing the evolution of the SL of the larvae according to the age expressed in dph. The two colors correspond to the age classes whose growth is contrasted in panel B. B: Table showing the correlation between the quantitative variables. SL is well correlated to developmental ages, and all quantitative traits are correlated to the standard length. C: Graph representing the growth of several quantitative traits according to standard length. BD, body depth; BH, body head; dph, days posthatching; ED, eye diameter; HL, head length; SAL, snout anal length; SL, standard length; SnL, snout length

for the second) (Figure 3A). Clownfish larvae thus accelerate their growth after 7 dph in our rearing condition. To determine if standard length (SL) is a better indicator than absolute age (dph) for larval developmental progress in *A. ocellaris*, we tested the difference between the correlation coefficients (R^2) of each developmental trait (head depth, body depth, head length, eye diameter, snout length, snout anal length) (see Figure 4A) against absolute age and SL. We used a paired Wilcoxon signed-rank test, as previously performed for Zebrafish larvae.⁴⁶ This analysis revealed that SL is a better indicator of developmental progress than age, as the mean R^2 for SL is higher than for dph (P value = 0.03, mean R^2 : dph = 0.90; SL = 0.96 mm) (Figure 3B). We therefore used SL as a proxy to describe the quantitative developmental progress in *A. ocellaris* larvae. However, it seems there are no differences in the predictive abilities of age and SL to describe qualitative criteria used to characterize the morphological changes of *A. ocellaris* larvae (P value = 0.31, mean R^2 : dph = 0.5; SL = 0.6) (Table 2). As expected, all quantitative traits were significantly correlated to SL (P value < 2.2×10^{-6} , R^2 ranging between 0.86 and 0.99) (Figure 3C). All these quantitative traits increase linearly at different rates,

with eye diameter and snout length being the parameters with the lowest slopes (eye diameter = $0.1 \times SL + 0.2$; snout length = $0.1 \times SL + 0.1$) (Figure 3B). The growth of head depth, body depth, head length, eye diameter, snout length, and snout anal length according to SL are shown in Figure 3C.

3.2 | Head development

At 1 dph, larvae show a rounded head (Figure 5A,B). It becomes progressively more triangular on the dorsal part between 1 dph and 4 dph, with the quadrate/mandible articulation becoming more rostral (Figure 5C–E). The lower jaw becomes more prominent from 4 to 10 dph (Figure 5C–E). There is no marked change in mouth position during these stages. As mentioned above, head length (HL) is significantly correlated with SL, measuring 1.3 mm (± 0.03 mm) at 1 dph (mean SL = 3.7 ± 0.5 mm) and reaching a maximum size of 3.6 mm (± 0.3 mm) at 30 dph. Compared to SL, HL grows slowly and constantly across to the two age classes determined above (mean growth rate = 0.06 mm/day from 1 to 7 dph, and 0.06 mm/day from 8 to 21 dph) (see Figure 3C). Eye diameter increases gradually, measuring 0.5 mm (± 0.01 mm) at 1 dph and reaching a

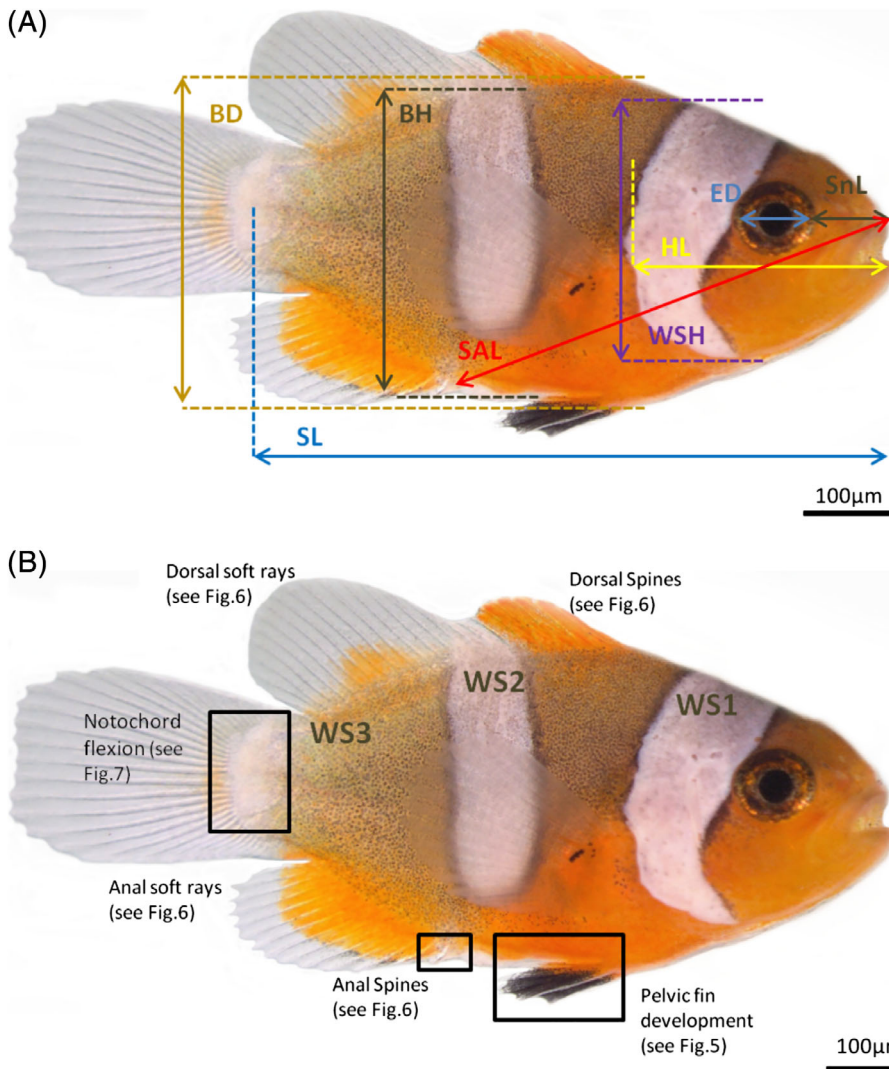


FIGURE 4 Quantitative and qualitative traits. Quantitative traits (A) and qualitative traits (B) used to describe clownfish postembryonic development. BD, body depth; BH, body head; ED, eye diameter; HL, head length; SAL, snout anal length; SL, standard length; SnL, snout length; WS, white stripe

TABLE 2 Predictive abilities of dph^a and SL^b for qualitative traits

| Trait | $dph R^2$ | $SL R^2$ |
|------------------------------|------------|------------|
| Anal soft rays | 0.6 | 0.4 |
| Anal spines | 0.6 | 0.7 |
| Dorsal soft rays | 0.6 | 0.5 |
| Dorsal spines | 0.7 | 0.9 |
| Pelvic fin | 0.6 | 0.7 |
| White stripe transparency | 0.5 | 0.4 |
| Caudal peduncle white stripe | 0.5 | 0.6 |
| Notochord flexion | 0.5 | 0.6 |

^adays posthatching.

^bstandard length.

maximum size of 1.2 mm (\pm 0.1 mm) at 30 dph. Eye growth is constant through development, with a mean growth rate of 0.014 mm/day from 1 to 7 dph, and 0.01 mm/day from 8 to 21 dph. The eye grows allometrically relative to the head, occupying 39% of the head surface at 1 dph and 30% at 21 dph.

3.3 | Fin development

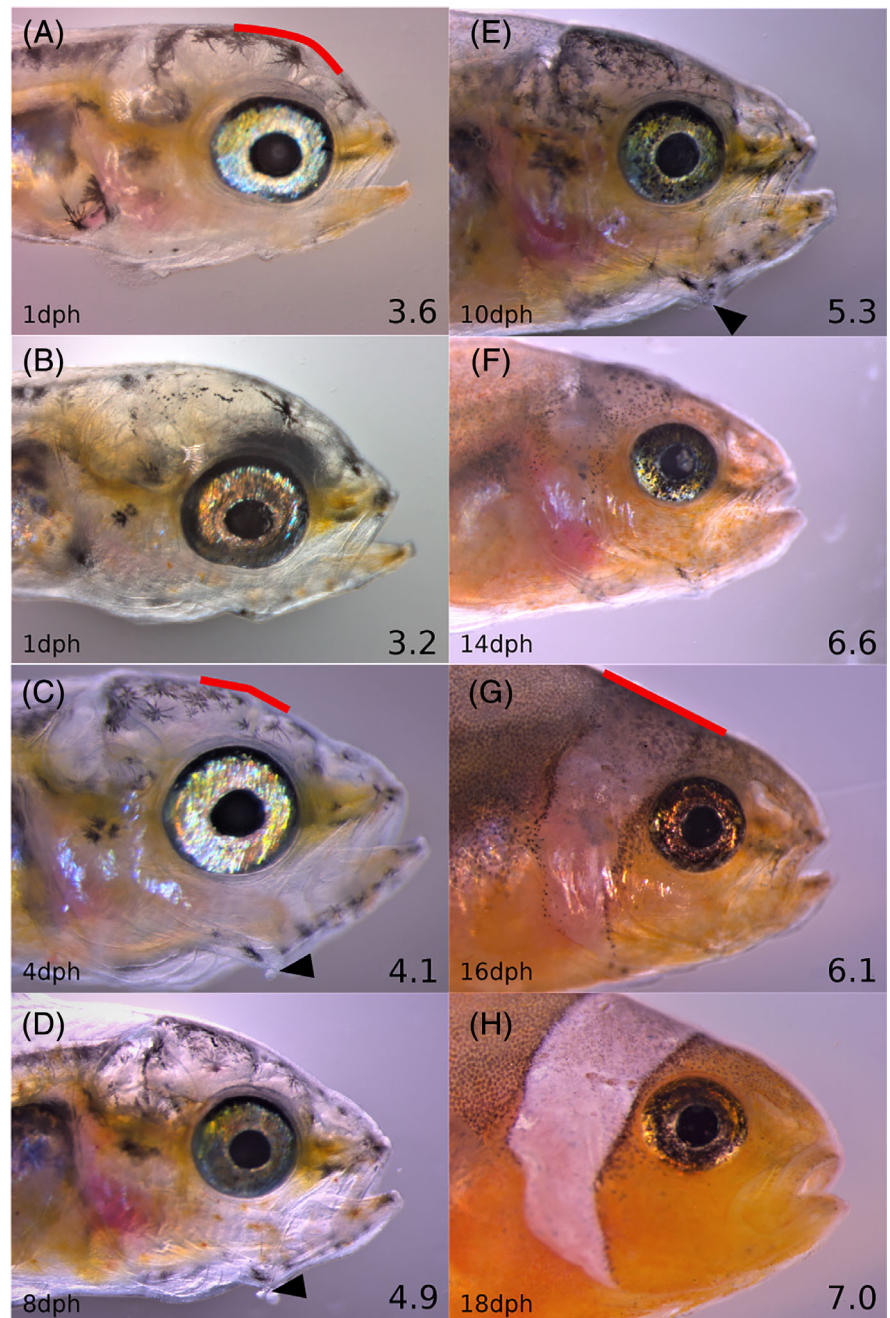
3.3.1 | Pectoral fins

Pectoral fins must be manipulated with forceps under a stereomicroscope to be distinctly observed. Therefore, we decided not to use them as a criterion for stage identification. Further, these fins are already formed at hatching; hatching clownfish are immediately able to swim and orient themselves using these fins. Consequently, our description of fin development focuses on pelvic fins and unpaired fins.

3.3.2 | Pelvic fins

The paired pelvic fins are located ventrally. They consist of one spine and three soft rays in adults. We categorize larval development of these fins into four steps (Figure 6A–D). We first observe no sign of fins (Figure 6A). Then a small bud appears between 2 dph and 8 dph (see black arrowheads on Figure 6B). This bud then develops into pelvic fins between 5 dph and 10 dph (black arrowhead on Figure 6C–E). The fins continue to grow and mature, and

FIGURE 5 Head development. A-H: Pictures of head during larval development at different ages indicated at the left of each panel. Red lines indicate the changes of shape of the dorsal part of the head, which is round at 1dph (A), then angular at 4 dph (C), and finally right at 16 dph (G). Black arrows heads indicate the lower jaw which is clearly visible between 4 and 10 dph (E). dph, days posthatching



finally, from 7 dph, pelvic spines start to appear (black arrowhead on Figure 6D,E).

3.3.3 | Unpaired fins

In *A. ocellaris*, dorsal and anal fins consist of spines (10-11 and 2 spines per fin, respectively) and soft rays (13-17 and 11-13 rays per fin, respectively). At 1 dph, larval tails are bordered by an embryonic fin fold, which is composed of three major lobes positioned ventrally at the posterior margin of the anus, dorsally at the rear quarter of the body, and ventrally surrounding the posterior tip of the notochord (Figure 7A). Within the ventral and dorsal lobes,

mesenchyme condensations (Figure 7A) mature into the soft tissue between the rays and spines. During development, the fin fold differentiates as unpaired fins and regresses at the caudal peduncle (Figure 7B).

Anal soft rays appear between 2 and 3 dph (orange arrowhead, Figure 7E,O); anal spines appear from posterior to anterior between 5 and 7 dph (blue arrowhead, Figure 7F). The anal fin is composed of a single major lobe (see Figure 7C).

Dorsal soft rays appear after anal ones between 3 and 4 dph (orange arrowheads on Figure 7H,I,O), but generally we observed that anal and dorsal soft rays appear at the same time. Dorsal spines appear also after anal ones, between 6 and 8 dph (indicated by blue arrowhead on Figure 7M-O). As anal

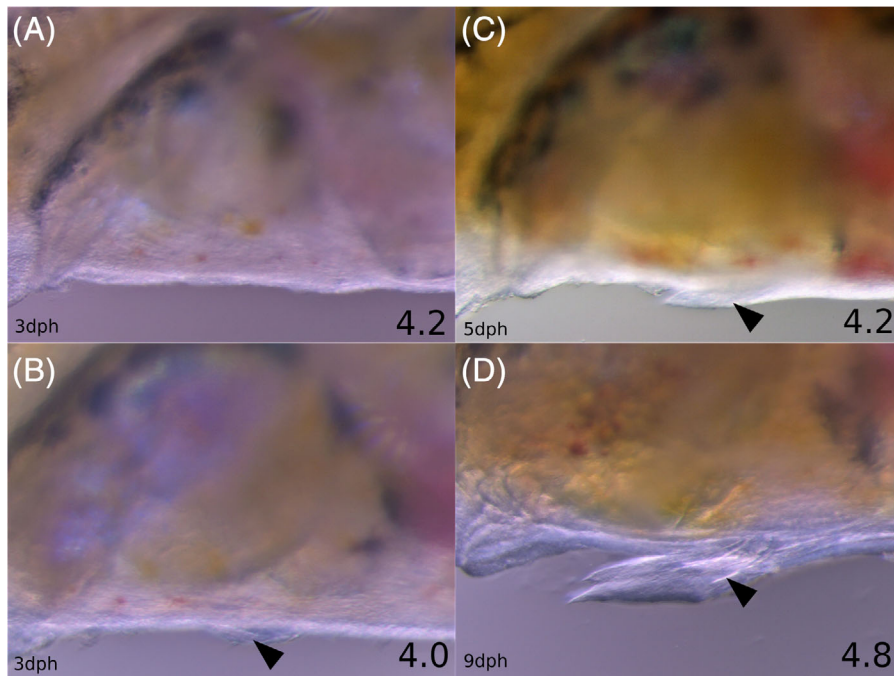
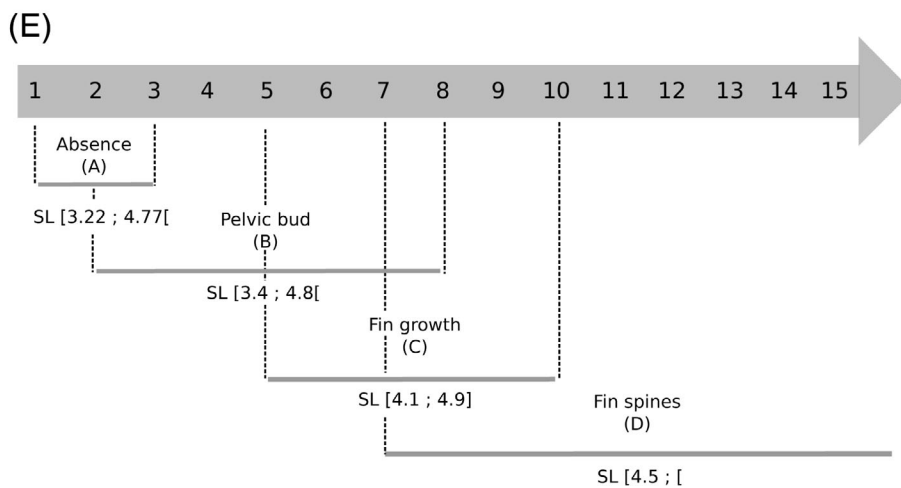


FIGURE 6 Changes of pelvic fin morphology through the postembryonic development. Photograph of pelvic fins at 3 dph (A), 3 dph (B), 5 dph (C), and 9 dph (D). We observe appearance of the pelvic fin bud (indicated by a black arrow in B). C: Growth of the pelvic fin (indicated by a black arrow). D: Appearance of the pelvic fin spines (indicated by a black arrow). E: Timescale showing the chronological appearance sequence of the different morphological traits of the pelvic fin. Dph, days posthatching; SL, standard length



spines, dorsal spines appear caudorostrally. The dorsal fin is composed of an anterior lobe supporting the spines and a posterior one supporting the soft rays (Figure 7C,G–N).

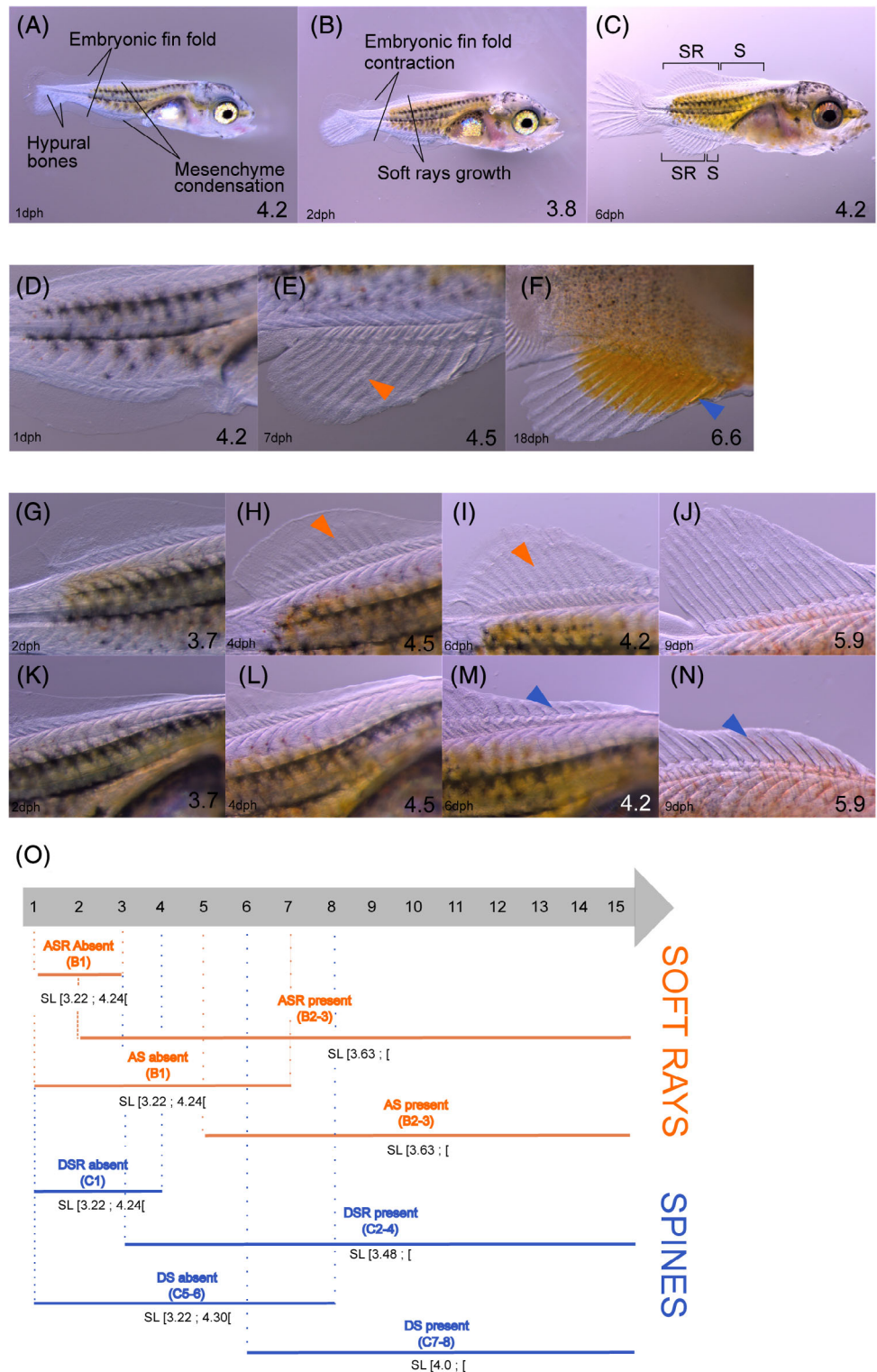
The caudal fin is composed of soft rays growing out of two hypural bones: a superior one and an inferior one (visible in Figure 8A). The development of the caudal fin is characterized by the flexion of the notochord and the formation of the rays. The flexion corresponds to a dorsal bending of the notochord. It normally ends when the hypural bones are in a vertical position as shown at 6 dph (Figure 8C). Thus, the notochord flexion is defined by three levels: preflexion, corresponding to a linear notochord (Figure 8A, 1 and 2 dph); flexion (Figure 8B, 2 and 3 dph); and postflexion (Figure 8C, 6 and 8 dph). The measure of the flexion angle was not taken at each developmental age as it is difficult to get a reliable measure once the caudal fin is pigmented. Thus, the postflexion levels are characterized by the vertical position of the hypural bones as shown in Figure 8C.

3.4 | Pigmentation

We focused on the development of the three major chromatophores in *A. ocellaris*: the black melanophores, the orange xanthophores, and the white iridophores.³⁰

Early posthatching larvae are lightly pigmented; their bodies are covered by two horizontal lines of stellate melanophores (Figure 9A). The dorsal line extends from the snout to the posterior extremity of the future dorsal fin (Figure 9A1,A2 and dorsal lines are indicated by black arrowhead on Figure 9A3). The ventral line extends from the trunk to the posterior extremity of the future anal fin (Figure 9A1,A2 and with black arrowhead on Figure 9A3). Both lines stop before the caudal peduncle (indicated by a black bar on Figure 9A1). Stellate melanophores are also spread on the body surface between those two lines, below the ventral line, above the internal organs (Figure 9C), and a few scattered dorsally over the head (Figure 9A4). Xanthophores

FIGURE 7 Changes of anal and dorsal fin morphology through the postembryonic development. A–C: Photographs of larvae at 1, 2, and 3 dph, respectively, highlighting dorsal and anal fin development. D–F: Anal fin development. We can observe appearance of soft rays (D) and spines (D, red arrowhead). G–N: Dorsal fin development with a focus of the soft rays (G–J) and spines (K–N). Orange arrowheads indicate soft rays, and blue arrowheads indicate spines. (O) Timescale showing the sequence of chronological appearance of the different anal and dorsal fin morphological traits. The soft rays (orange) and spines (blue) are separated for clarity. AS, anal spines; ASR, anal soft rays; DS, dorsal spines; DSR, dorsal soft rays; S, spines; SR, soft rays



extend from the snout (yellow arrowhead in Figure 9A4) to the posterior extremities of both future anal and dorsal fins, giving the larval body its yellow coloration. Some xanthophores are also found above the swim bladder (yellow arrowhead in Figure 9A2); this region is also covered by iridophores (indicated by a black arrow, Figure 9A1).

Up to 9 dph, the same overall pattern is observed: Melanophores form two lines and are scattered across the body and the

head (illustrated in Figure 9B1 with a 6-dph larva). The yellow coloration increases during this period, with xanthophores extending across the body surface (Figure 9B2,B3). Xanthophores are still present on the head (yellow arrowheads, Figure 9B4). The caudal peduncle remains transparent (Figure 9B1).

From 9 dph, the larval coloration changes from yellow to orange (see 10-dph larva in Figure 9C, and 14-dph larva in Figure 9D). Orange xanthophores start to cover the ventral and

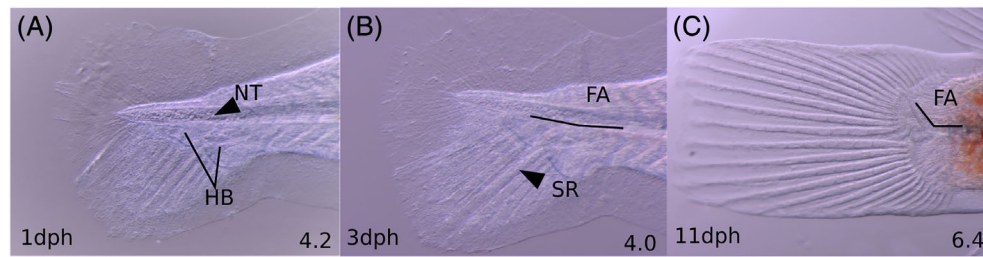


FIGURE 8 Caudal fin development throughout larval development. A–C: Stereomicroscope pictures of the caudal fin showing the preflexion stage (1 dph, A), the flexion stage (3 dph, B), and the postflexion stage (11 dph, C). Flexion stage starts when the notochord starts to bend and hypural bones tend to get a vertical position. Postflexion stage is reached when the hypural bones are in vertical position. Dph, days posthatching; FA, flexion angle; HB, hypural bones; NT, notochord; SR, soft rays

dorsal parts of the body, getting closer to the anal and dorsal fins and extending on the head (Figure 9C2,D2, orange arrows). Fins remain unpigmented until after 10 dph (Figure 10A–C). The caudal peduncle also remains unpigmented (Figure 10A). The white stripes of the body and the head start to appear in 14-dph larva (Figure 9D1). The white stripe of the body is dorsally located below the last three spines of the dorsal fin (visible in Figure 10O, black arrows showing the three spines), and it is ventrally located above the cloaca (Figure 9F1, black arrow indicating the cloaca). During the formation of these white stripes, we can observe a concentration of black melanophores on the border (indicated by black arrows on Figure 9D2–F2). The white stripes are first transparent (Figure 9D1,E1) before becoming fully white (Figure 9F1,G1). The head and body stripes are the first to appear (between 9 and 14 dph); the third stripe on the caudal peduncle appears later, at ~17 dph. When the white stripes appear, the two horizontal lines of melanophores progressively fade (Figure 9D2–G2). The orange xanthophores appear on the anal and dorsal fins (indicated by red arrowheads in Figure 10E,F,H,J), and on the caudal peduncle (Figure 10G). The caudal fin is the last of the fins to remain unpigmented. Orange xanthophores cover the base of the caudal fin, close to the white stripe (Figure 10P, red arrowhead), black melanophores surround the xanthophores, and the extremity of the fin remains transparent.

3.5 | Tooth and sensory organ development

To follow the development of teeth and sensory organs, *A. ocellaris* larvae were observed under a scanning electron microscope (Figure 11). Hatching larvae initially lack teeth (Figure 11A). The first teeth appear at 9 dph (white arrow, Figure 11B). They are canine-type teeth typical of carnivorous fish like *A. ocellaris*. They are covered by a layer of epithelial cells (Figure 11D) that are eventually perforated as the teeth grow, as shown in Figure 11C,E in a 12-dph larvae.

For the appearance of sensory organs, we focused on the description of olfactory placodes and the system of the lateral line, which is composed of five types of sensory canals distributed on the head and the body. At 1 dph, olfactory

placodes are triangular and are covered by a layer of ciliated cells (Figure 11F). At 6 dph, this placode invaginates and its border merges to form two openings corresponding to the nostrils (Figure 11G). Their formation is completed when the two nostrils are fully separated, as shown on Figure 11H in a juvenile.

Sensory canals of the head are absent at 1 dph (Figure 11J). At 11 dph, the supraorbital, temporal and opercular canals are forming. Their formation corresponds to an invagination of neuromasts (Figure 11I). They will finally have the appearance of holes surrounding the eye (infra- and supraorbital canals), above the head (temporal canals), distributed along the opercular (opercular canals), and below the mandible (mandibular canals) (Figure 11L,M).

The lateral line appears at 6 dph (Figure 11O) with the appearance of neuromasts (Figure 11R), which invaginate to form the head sensory canals (Figure 11P,S).

3.6 | Description of qualitative traits used to identify the developmental stages

Eight qualitative traits were chosen to identify developmental stages: the notochord, dorsal soft rays, anal soft rays, dorsal spines, anal spines, pelvic fins, head white stripe, and caudal white stripe (Figure 3B; Table 1). Each of these selected traits is categorized into two or three categories. For example, the notochord goes through the following steps: preflexion (Figure 8A), flexion (Figure 8B), and postflexion (Figure 8C). Soft rays and spines appear sequentially in the anal and dorsal fins, which is why we define them as distinct criteria based on their appearance (Figure 7). Soft rays invariably appear before spines in both the dorsal and anal fins. Pelvic fin development has four distinct steps: absent (Figure 6A), pelvic bud (Figure 6B), pelvic fin (Figure 6C), and pelvic spines (Figure 6D). Finally, head and caudal fin white stripes appear sequentially (Figure 9). The head white stripe is categorized as absent (Figure 9A1–C1), transparent (Figure 9D1,E1), or present (Figure 9F1,G1), contrary to the caudal white stripe, which is categorized only as absent (Figure 9A1–F1)

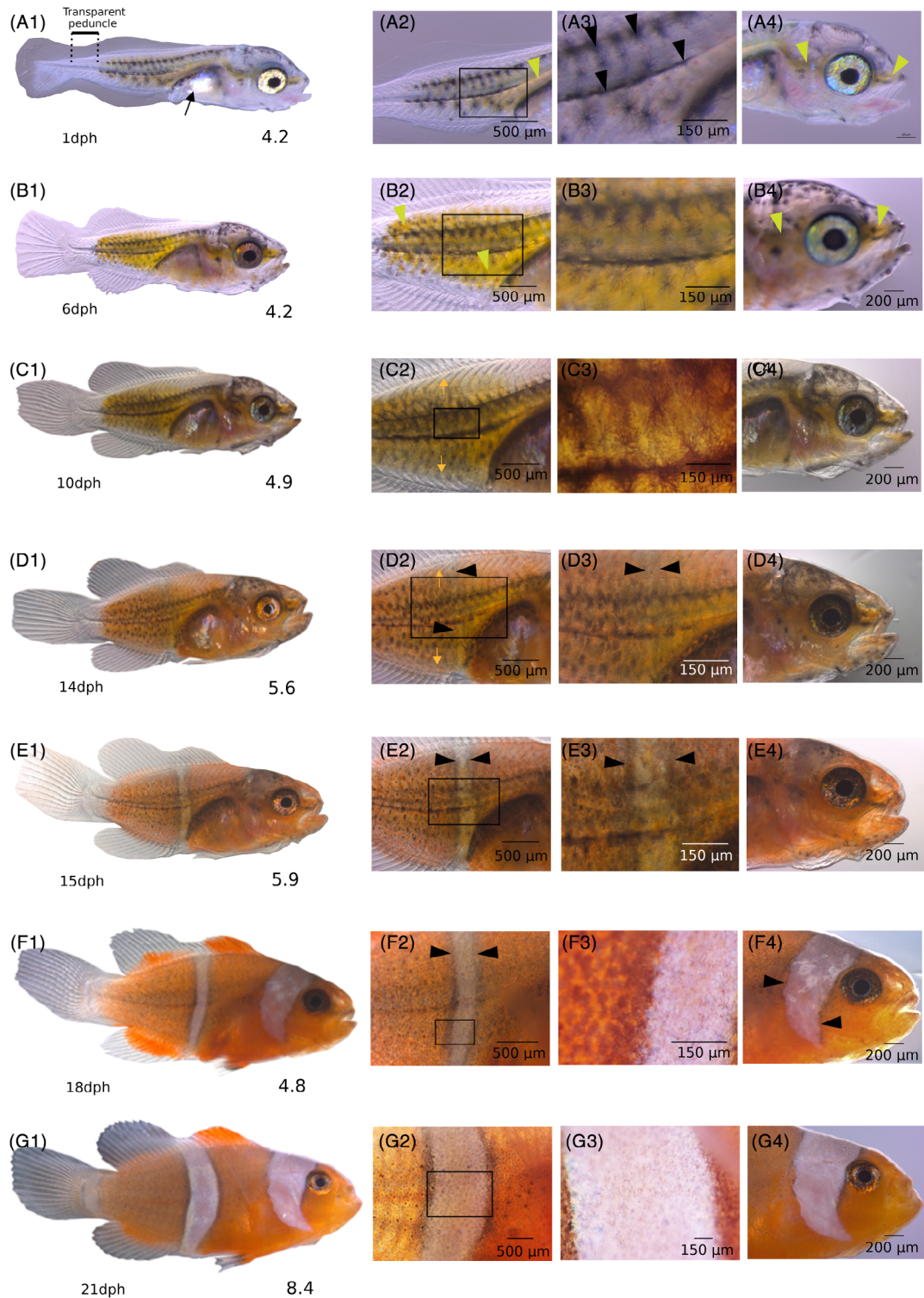


FIGURE 9 Body pigmentation throughout larval development. A1–G1: Pictures of larvae from 1 dph to 21 dph. Close-ups on the central body (A2–G2), pigment cells (A3–G3), and heads (A4–G4). Black and yellow arrowheads indicate, respectively, stellate melanophores from the horizontal lines covering the larval body and xanthophores that are dispersed on the larval body. Black squares indicate the zone highlighted on the third column. Orange arrows indicate orange xanthophores also forming round cells. Black arrowhead indicates metamorphic melanophores invading the flank of *Amphiprion ocellaris* that concentrate on the margin part of the white stripes

or present (Figure 9G1). To define developmental stages, individuals were categorized according to the chronological appearance of the different criteria. This allows us to define

seven distinct developmental stages. Table 3 summarizes the criteria we use to characterize each developmental stage.

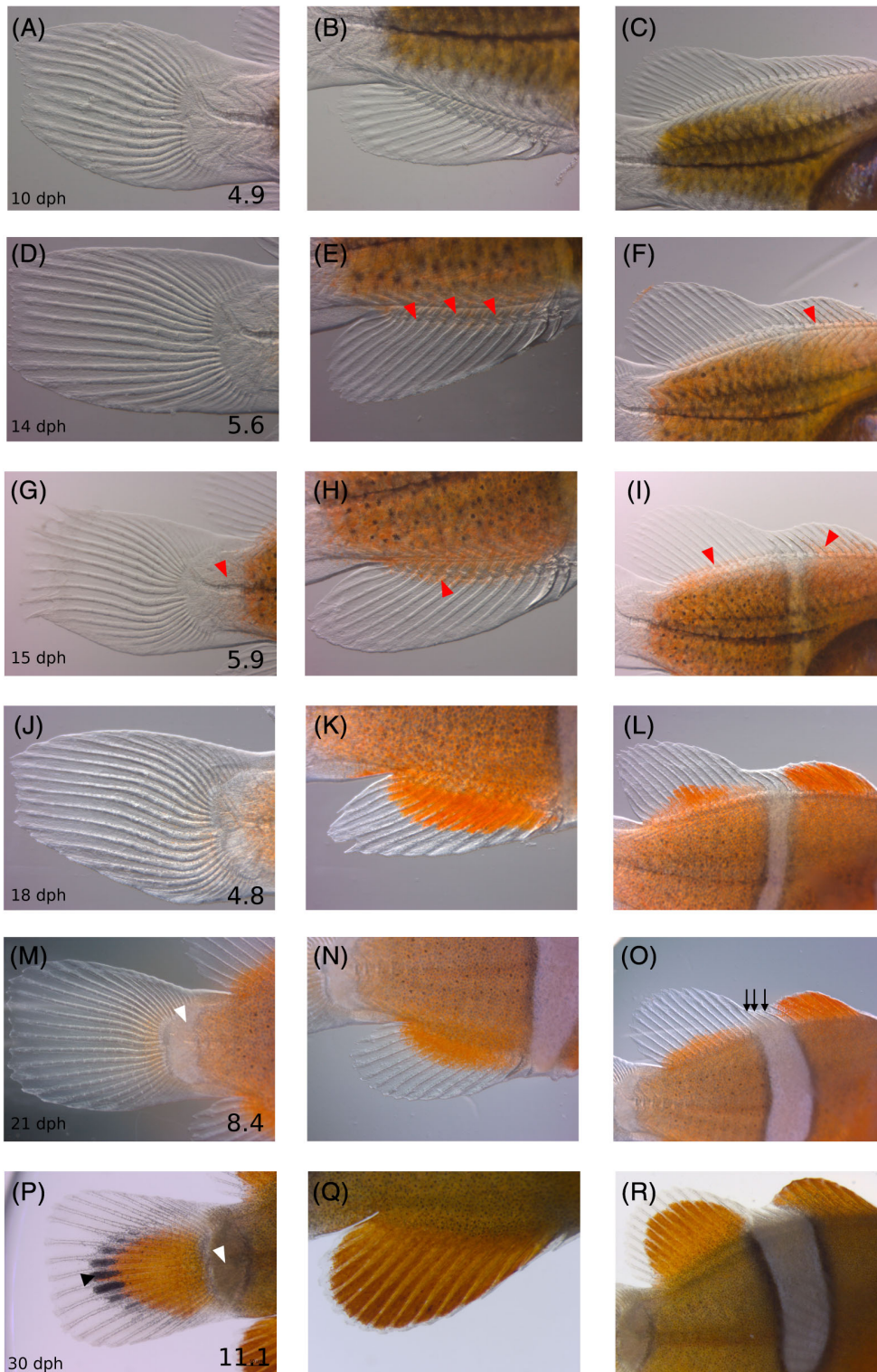


FIGURE 10 Fins pigmentation throughout larval development. Left column: Caudal fin development from 10 dph (A) to 30 dph (P), with orange xanthophores progressing on the caudal peduncle at 15 dph (G, red arrowhead) and white stripe appearing at 21 dph (M, white arrowhead). Middle column: Anal fin pigmentation, which starts at 14 dph (E, red arrow head). Right column: Pigmentation of the dorsal fin, which appears at 14 dph (F, red arrowhead). Black arrowheads on G indicate the spines behind the body white stripe. The age in dph is indicated on each picture of the first columns and is valid for all the respective horizontal series. Dph, days posthatching

3.7 | The postembryonic developmental stages

Below, we describe the characteristics of each stage and illustrate with representative individuals (Figures 12–18). *Italic terms correspond to the qualitative criteria used to identify the different stages; bold terms correspond to the criteria allowing the distinction between two developmental stages.*

3.7.1 | Stage 1: Preflexion stage (Figure 12)

This stage corresponds to larvae between 1 and 3 dph. A transparent embryonic fin fold surrounds the larval body and tail (Figure 12A,F, black arrowhead). *Larvae have no anal or dorsal fin rays or spines* (Figure 12A,B,E,F). *The pelvic fin is absent but a bud may be present* (Figure 12D, black arrowhead). The yolk is entirely absent, and larvae

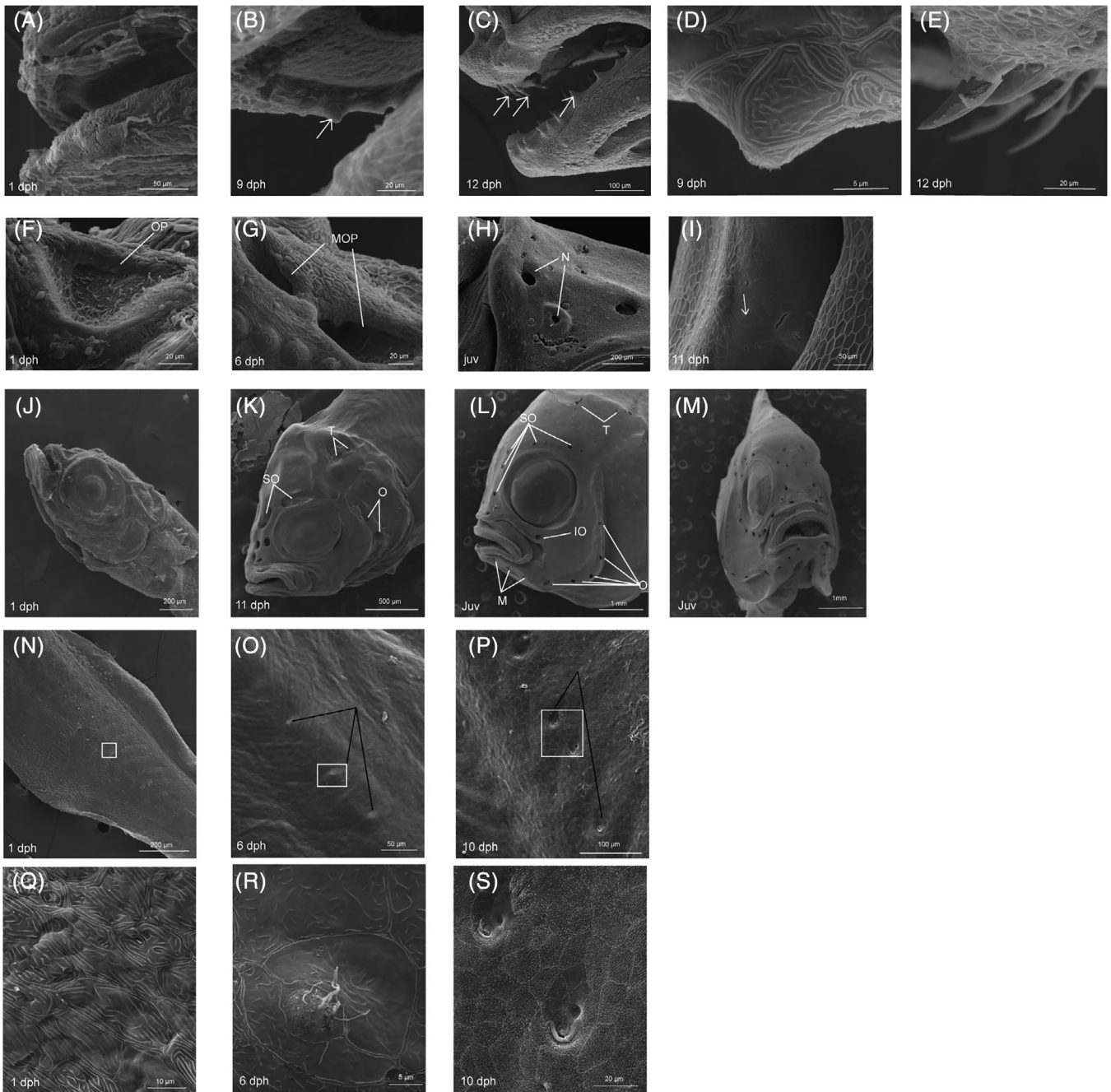


FIGURE 11 Tooth and sensory organs. Development of tooth and sensory organs observed by scanning electronic microscopy. A–E: Appearance of the tooth (white arrow), and in E, teeth breaking epithelial cells at 12 dph. F–I: Development of the nostrils (white arrows), and in I, close-up on the invagination of a neuromast in a sensory canal (indicated by a white arrow). J–M: Development of head sensory canals, and in M, the frontal view of the sensory canals covering the head of a juvenile. N–P: Development of the body lateral line. Q–S: Close-up of the zones indicated in N, O, and P. dph, days posthatching; IO, infra-orbital canals; Juv, juvenile; M, mandibular canals; MOP, merging olfactory placodes; N, nostrils; O, opercular canals; OP, olfactory placodes; SO, supraorbital canals; T, temporal canals

have open mouths and are able to feed on live prey (Figure 12C). The pigmentation is composed of two lines of melanophores on the body (Figure 12A,B, black arrowhead); some melanophores are scattered on the head, and some xanthophores cover the body and the head (Figure 12C). Iridophores are visible above internal organs (white arrows, Figure 12I,C) and behind the eye (white

arrow, Figure 12C). *The white stripes of the head and the caudal fin are absent* (Figure 12C,I). The swim bladder is difficult to see as it is hidden by a layer of melanophores (indicated by a black arrow in Figure 12B) and shiny iridophores (Figure 12I). The **notochord is in preflexion** (indicated by a black arrowhead in Figure 12G), and hypural bones support growing caudal rays (black arrows,

TABLE 3 Qualitative traits characterizing each development stages^a

| Developmental Stages | Notochord | Anal soft rays | Anal spines | Dorsal soft rays | Dorsal spines | Pelvic fin | Head and body white stripes | Caudal fin white stripe |
|----------------------|--------------------|----------------|-------------|------------------|---------------|---------------|-----------------------------|-------------------------|
| 1 | Preflexion | Absent | Absent | Absent | Absent | Absent/Bud | Absent | Absent |
| 2 | Flexion | Present | Absent | Present | Absent | Bud | Absent | Absent |
| 3 | Postflexion | Present | Present | Present | Absent | Bud/Fin | Absent | Absent |
| 4 | Postflexion | Present | Present | Present | Present | Spines | Absent | Absent |
| 5 | Postflexion | Present | Present | Present | Present | Spines | Transparent | Absent |
| 6 | Postflexion | Present | Present | Present | Present | Spines | White | Absent |
| 7 | Postflexion | Present | Present | Present | Present | Spines | White | Present |

^aBold terms correspond to criteria used to differentiate each stage from each other.

Figure 12H). Larvae of this stage exhibit swimming behavior; they are attracted to light and swim at the top of the water column.

3.7.2 | Stage 2: Flexion stage (Figure 13)

At this stage, larvae are between 2 and 8 dph. The body and tail are still surrounded by the embryonic fin fold, which has started to differentiate in the future dorsal and anal fins, with soft rays beginning to appear (Figure 13A, B,E,F, black arrowheads). Similarly, the caudal embryonic fin fold is differentiating in the caudal fin with rays still growing and the **notochord has begun to flex** (Figure 13G,H). *A pelvic bud is present* (Figure 13D, black arrowhead) and *anal and dorsal soft rays have appeared* (Figure 13A,F, black arrowhead). The larval body remains pigmented as in stage 1, but the layer of xanthophores has extended along the larval body and *white stripes remain absent* (Figure 13C,F).

3.7.3 | Stage 3: Postflexion stage (Figure 14)

Larvae of this stage are between 3 and 10 dph. The embryonic fin fold has completely differentiated into dorsal, anal, and caudal fins (Figure 14A,B,F,H). All *anal and dorsal soft rays are present* (anal soft rays appear between 11 and 14 dph; dorsal soft rays appear between 13 and 17 dph), giving the fins their final form (Figure 14A,F). *Dorsal and anal spines have appeared* (Figure 14B,E, black arrowhead). Spines appear brighter and are not segmented compared to soft rays (see Figure 14 A,B). *A pelvic bud is present and begins differentiating in fin* (Figure 14D, black arrowhead). We observed no change in the body and head pigmentation from the flexion stage, and still *no visible white stripes* (Figure 14B,H). In contrast to the flexion stage, **notochord is in postflexion** and hypural bones assume a vertical position (indicated in Figure 14A). At this stage, larvae still swim high in the water column and close to the surface of the water.

3.7.4 | Stage 4: Pelvic spine stage (Figure 15)

Larvae of this stage are between 5 and 14 dph. The body shape has changed, with the body deepening compared to previous stages. The fins are fully developed, and *anal and dorsal fin spines are present* (2 for the anal fin, and between 10 and 11 for dorsal fin, Figure 15A,B,E,F). **The pelvic fins have all their spines** (Figure 15D). *The notochord remains in postflexion* (Figure 15G,H). The two lines of melanophores are still present and xanthophores still cover the body up to the anal and dorsal fins. *The head and caudal fin white stripes are absent* (Figure 15C,F). At this stage, larvae swim close to the bottom and are no longer attracted to light.

3.7.5 | Stage 5: Two transparent white stripes stage (Figure 16)

At this stage, larvae are between 9 and 15 dph and have undergone major changes in pigmentation; all the other morphological traits used to identify developmental stages are in their final states (Table 2). The *anal and dorsal fins have all their soft rays and spines, and the notochord is in postflexion* (Figure 16A,B,D–H). The xanthophores have begun to cover the anal and dorsal fins, as well as the caudal peduncle. At this stage, yellow is replaced by an orange pigmentation. The two lines of melanophores have begun to disappear, but are still visible in most individuals. The head becomes orange and **the white head stripe is increasingly visible** (Figure 16C). At this stage, the stripe is transparent and surrounded by groups of melanophores (black arrows, Figure 16C). The **body white stripe also appears and remains transparent** at this stage. The white stripe of the body is always localized at the base of the posteriormost three spines of the dorsal fin, and the stripe reaches the cloaca (Figure 16I). The white stripe of the head is also bordered by melanophores (black arrows on Figure 16B). At this stage, there is no sign of the third white stripe that will be located on the caudal peduncle.

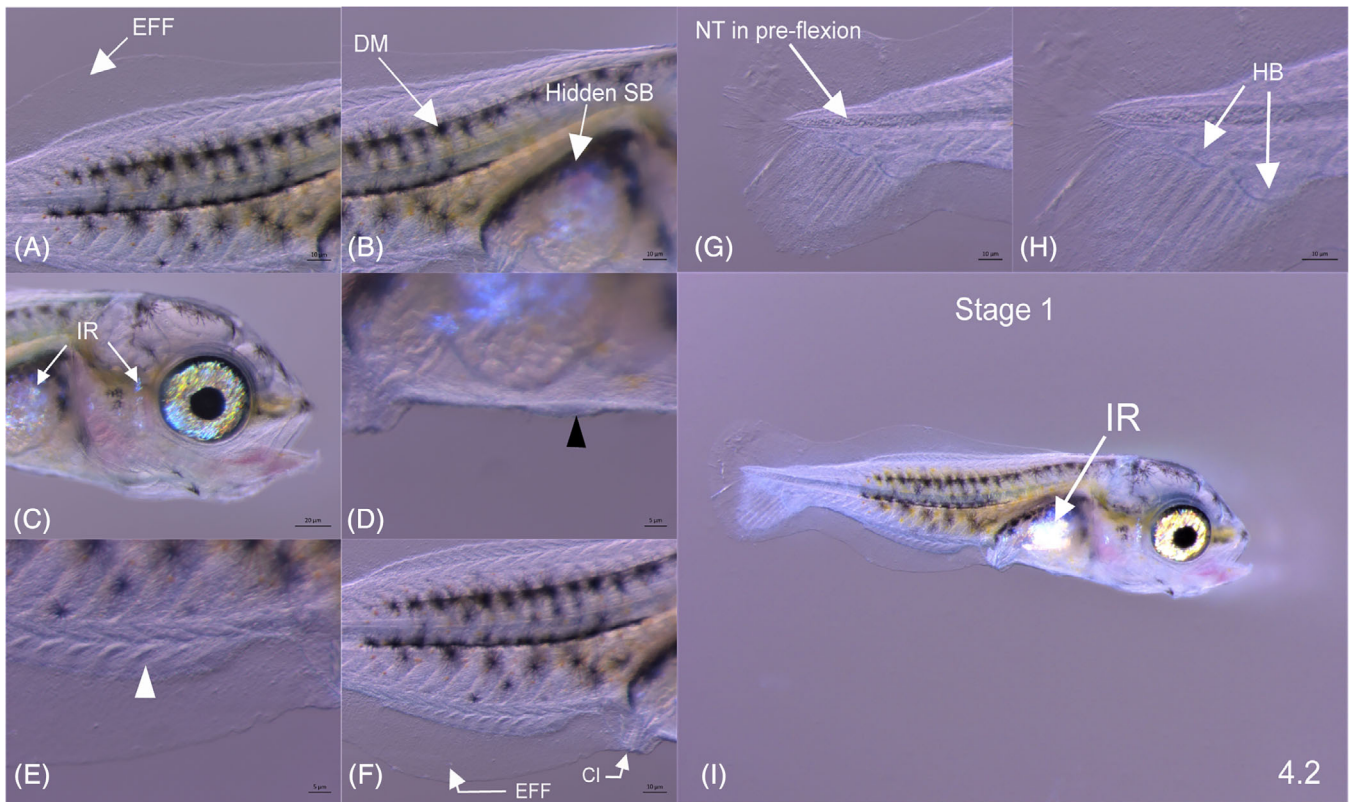


FIGURE 12 Preflexion stage larvae. A–I: Lateral views of the dorsal fin (A,B), the head (C), the pelvic fin (D), anal soft rays and anal fin (E,F), notochord and hypural bones (G,H), and whole body (I). Black arrowheads indicate pelvic bud (D) and the structure holding anal soft rays (E). Cl, cloaca; DM, dendritic melanophore; EFF, embryonic fin fold; HB, hypural bones; IR, iridophore; NT, notochord; SB, swim bladder

3.7.6 | Stage 6: Two white stripes stage (Figure 17)

This stage corresponds to larvae between 10 and 20 dph. The body shape changes, the body depth being higher than the previous stage. The pigmentation is more orange than the previous stage; the orange xanthophores have spread onto the anal and dorsal fins (Figure 17A,B,E,F) and they cover the base of the caudal fin. Some melanophores have begun to appear on the pelvic fins (black arrowhead of Figure 17D). **The white stripes of the head and the body become whiter and more opaque**, and their margins are still composed of melanophores. The stripes have grown and now reach to the ventral part of the body. The two horizontal lines of melanophores continue to disappear but are still visible in most individuals.

3.7.7 | Stage 7: Three white stripes stage (Figure 18)

At this stage, larvae are older than 17 dph. The body exhibits a juvenile oval shape and the pigmentation continues to mature. The lobe supporting the spines of the dorsal fin is the first to be fully pigmented (Figure 18B). The pelvic fins

are almost fully pigmented at this stage. They are primarily pigmented by melanophores at the extremity and by orange xanthophores at the base (Figure 18D). The orange xanthophores have extended on the anal fin and on the second lobe of the dorsal fin. The caudal fin remains mostly unpigmented. At this stage the white stripes of the head and the body are fully formed and outlined by melanophores. **The third white stripe appears at this stage on the caudal peduncle** (Figure 18F).

3.8 | A dichotomous key determination useful for staging

A dichotomous key determination based on multiple-choice questions has been created to assist users in identifying the various postembryonic developmental stages (Figure 19). Then, depending on the answer, the key indicates whether the user has to go to the next question or if the stage of its sample stage is identified. For example, if the larva being observed does not have a flexed notochord, it is stage 1. In contrast, if the larva has a flexed notochord, the user moves on to the next question. This key is used routinely in our laboratory and has been especially valuable for inexperienced users.

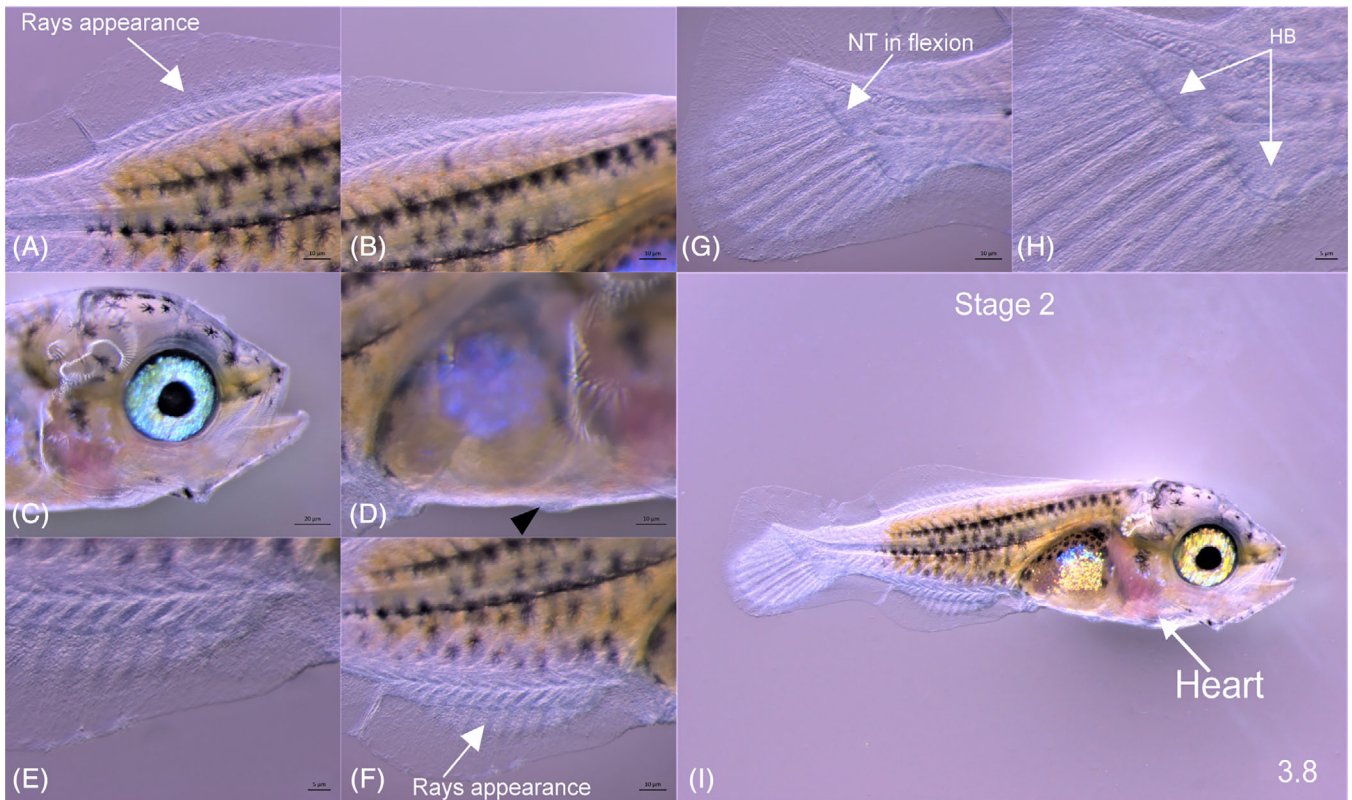


FIGURE 13 Flexion stage larvae. A–I: Lateral views of the dorsal fin (A,B), the head (C), the pelvic fin (D), anal soft rays and anal fin (E,F), notochord and hypural bones (G,H) and whole body (I). Black arrowheads indicate pelvic bud (D). HB, hypural bones; NT, notochord

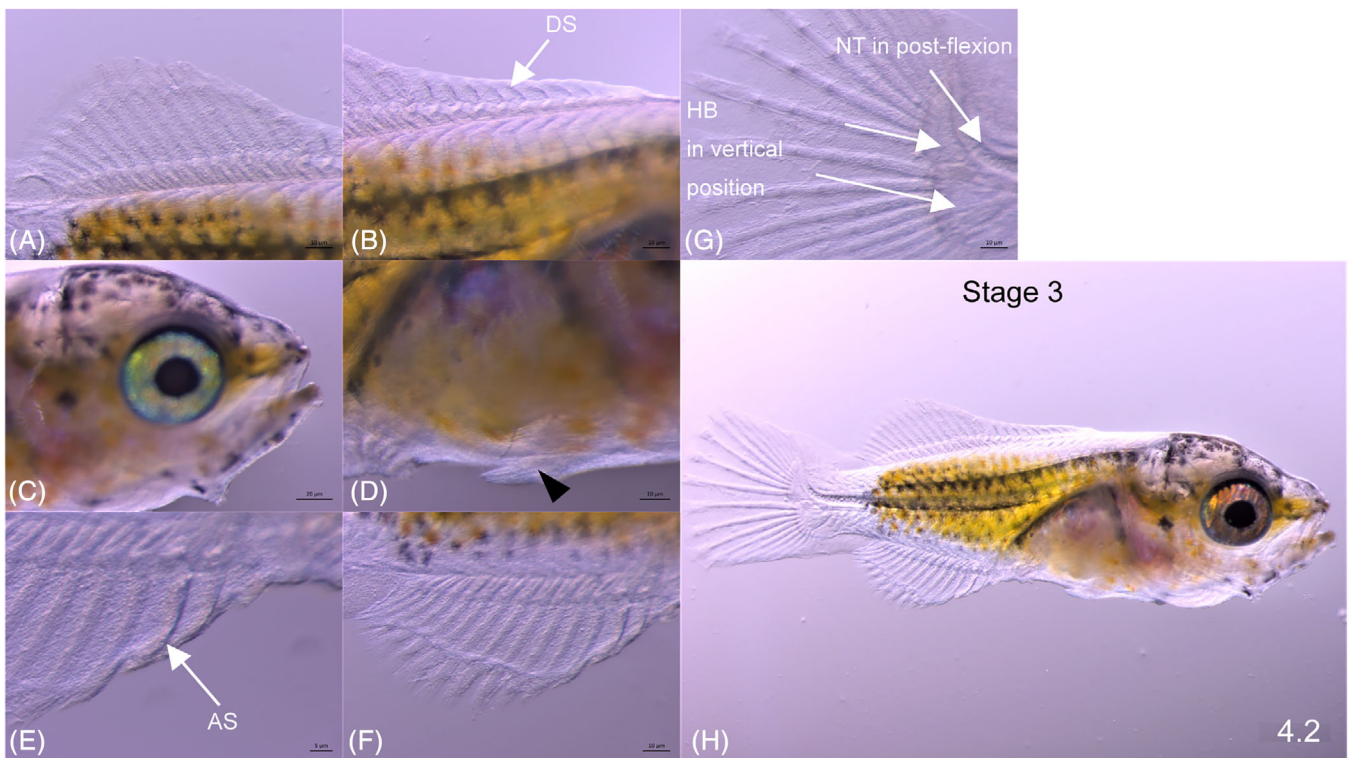


FIGURE 14 Postflexion stage larvae. A–H: Lateral views of the dorsal fin (A,B), the head (C), the pelvic fin (D), anal soft rays and anal fin (E,F), notochord and hypural bones (G), and whole body (H). Black arrowheads indicate pelvic bud (D). AS, anal fin spines; DS, dorsal fin spines; HB, hypural bones; NT, notochord

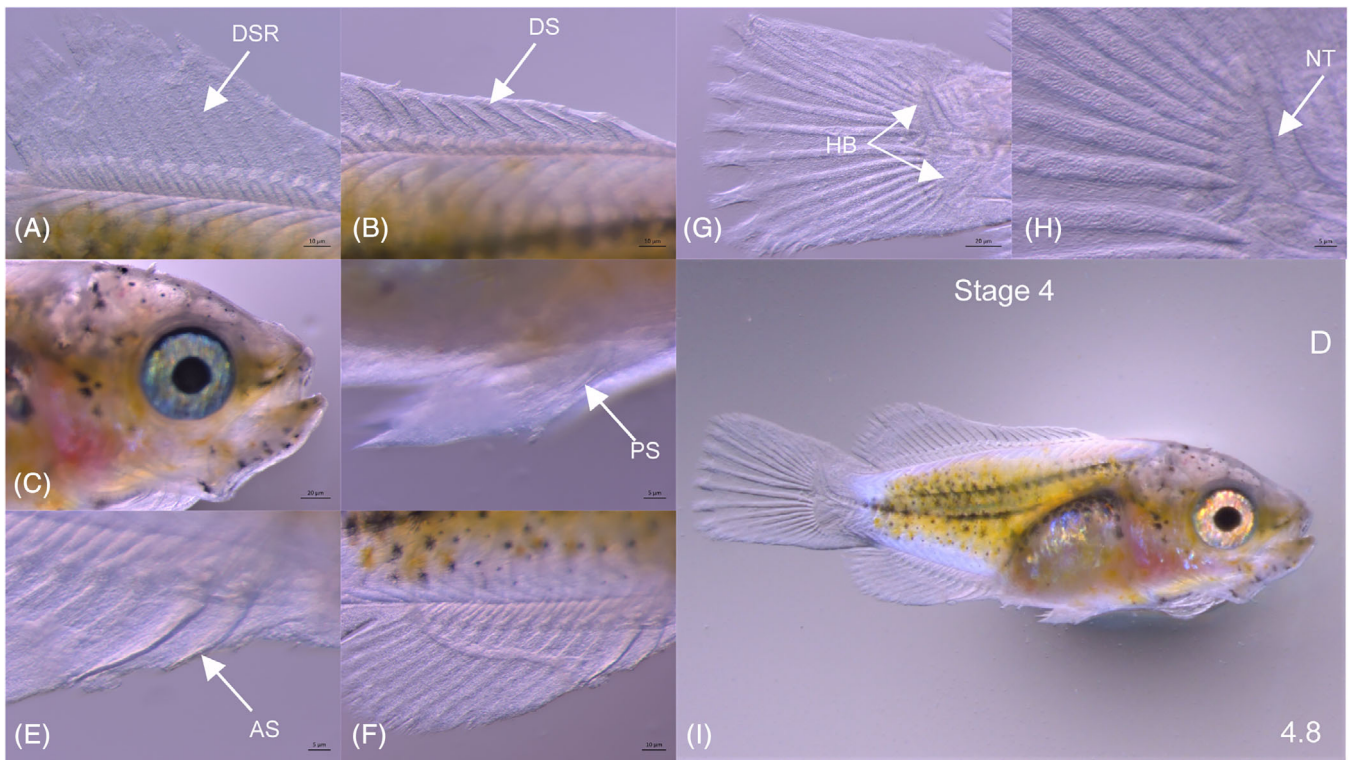


FIGURE 15 Pelvic spine stage larvae. A–I: Lateral views of the dorsal fin (A,B), the head (C), the pelvic fin (D), anal soft rays and anal fin (E,F), notochord and hypural bones (G,H), and whole body (I). Black arrowheads indicate pelvic bud (D). AS, anal spines; DS, dorsal spines; DSR, dorsal soft rays; HB, hypural bones; NT, notochord; PS, pelvic spines

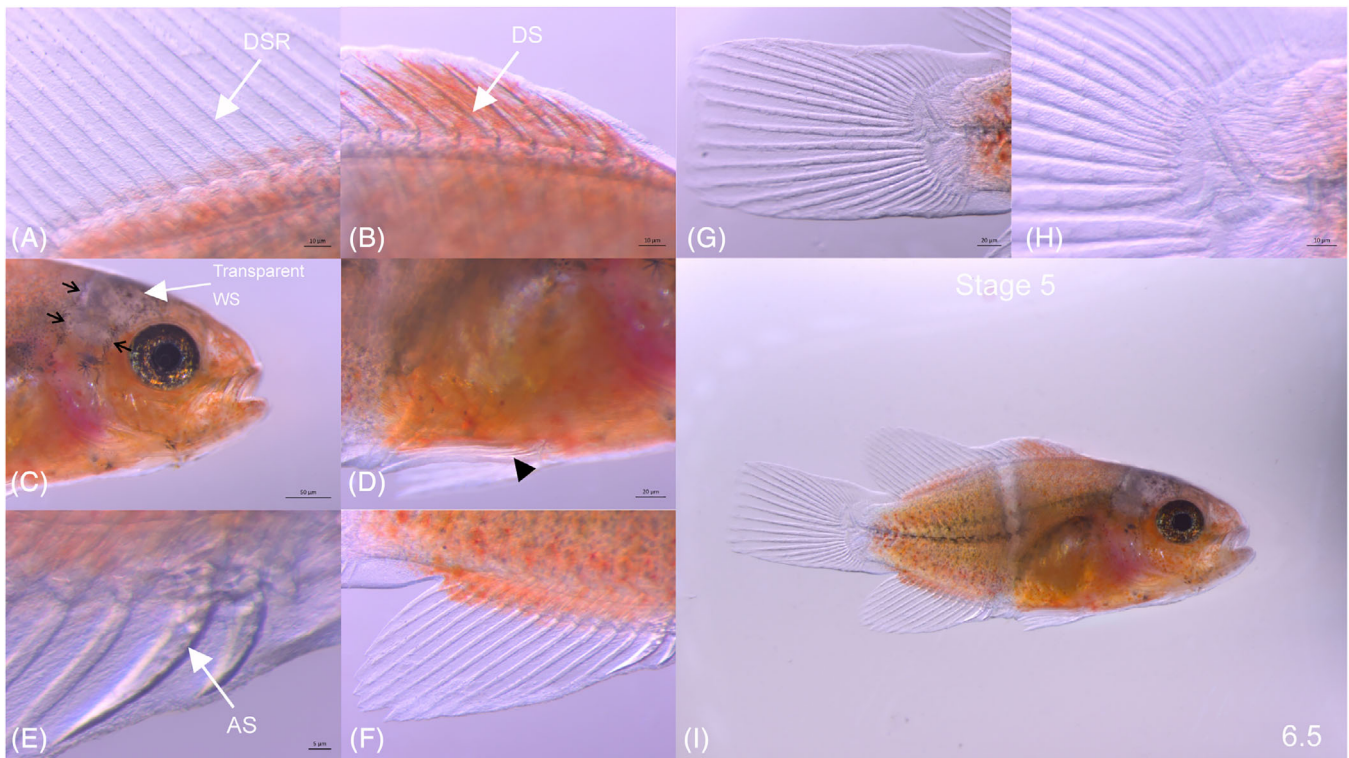


FIGURE 16 Two transparent white stripe stage larvae. A–I: Lateral views of the dorsal fin (A,B), the head (C), the pelvic fin (D), anal soft rays and anal fin (E,F), notochord and hypural bones (G,H), and whole body (I). Black arrows indicate the melanophores surrounding the transparent white stripe appearing on the head. Black arrowheads indicate pelvic bud (D). AS, anal spines; DS, dorsal spines; DSR, dorsal soft rays; HB, hypural bones; NT, notochord; PS, pelvic spines; WS, white stripe

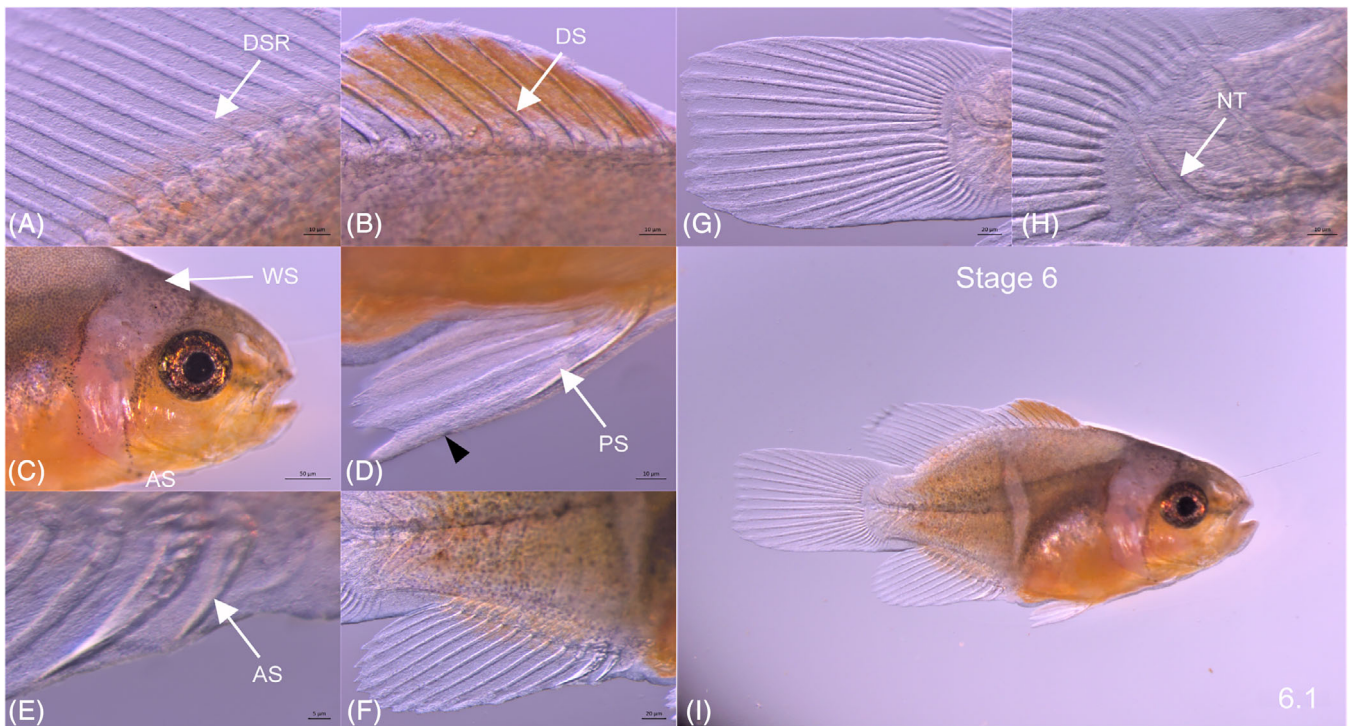


FIGURE 17 Two white stripe stage larvae. A–I: Lateral views of the dorsal fin (A,B), the head (C), the pelvic fin (D), anal soft rays and anal fin (E,F), notochord and hypural bones (G,H), and whole body (I). Black arrows indicate the melanophores surrounding the transparent white stripe appearing on the head. Black arrowheads indicate pelvic bud (D). AS, anal spines; DS, dorsal spines; DSR, dorsal soft rays; HB, hypural bones; NT, notochord; PS, pelvic spines; WS, white stripe

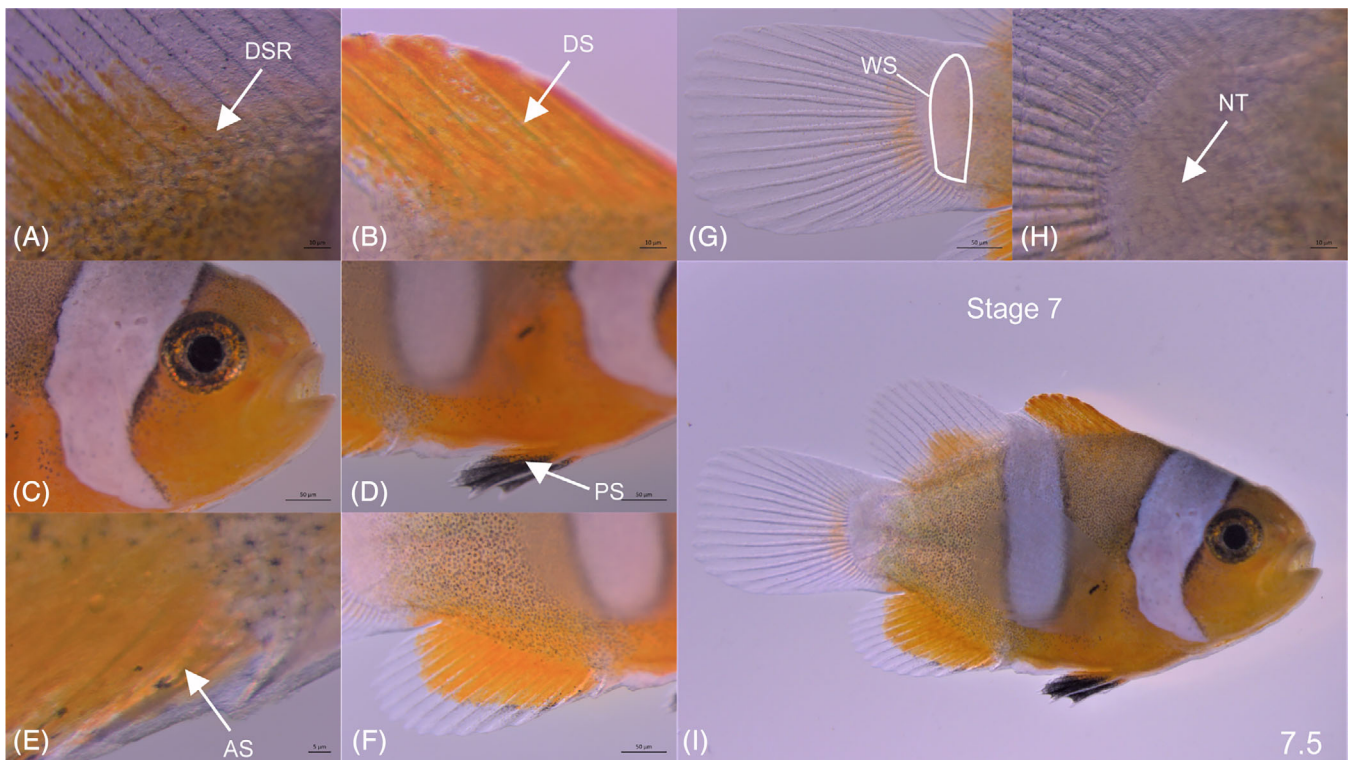


FIGURE 18 Three white stripe stage larvae. A–I: Lateral views of the dorsal fin (A,B), the head (C), the pelvic fin (D), anal soft rays and anal fin (E,F), notochord and hypural bones (G,H) and whole body (I). Black arrows indicate the melanophores surrounding the transparent white stripe appearing on the head. Black arrowheads indicate pelvic bud in (D). AS, anal spines; DS, dorsal spines; DSR, dorsal soft rays; NT, notochord; PS, pelvic spines; WS, white stripe

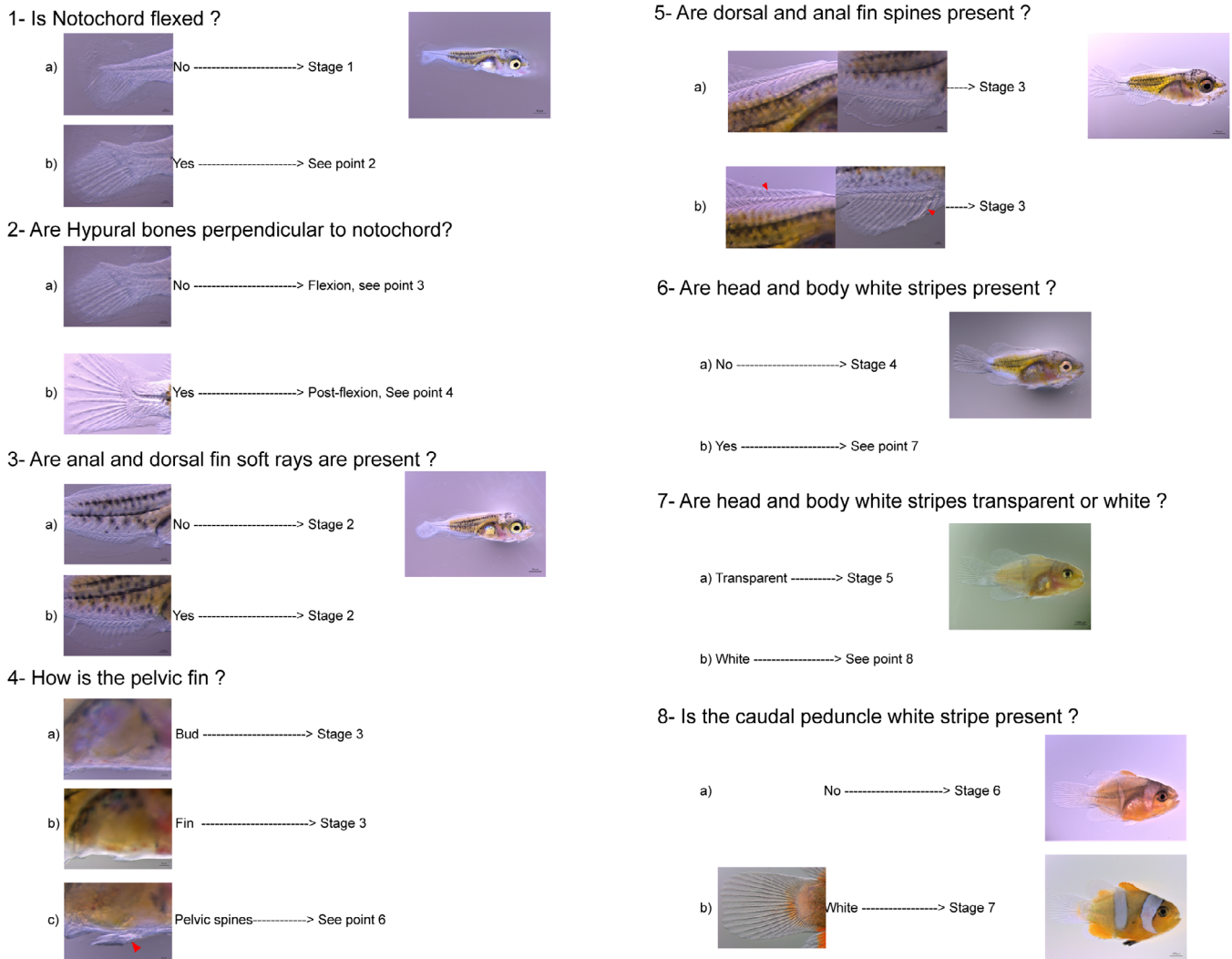


FIGURE 19 Key determination. Determination key of the developmental stages of *Amphiprion ocellaris* larvae

4 | DISCUSSION

In this study, we provided a detailed description and a staging system of the postembryonic development of the clownfish *A. ocellaris*. In particular, we described seven quantitative traits commonly used to follow fish larval development (standard length, head length, body depth, body height, eye diameter, snout length, and snout anal length)^{41,46,63-65} as well as eight qualitative traits (notochord, dorsal soft rays, anal soft rays, dorsal spines, anal spines, pelvic fin, head white stripe and caudal white stripe). Using these qualitative criteria, we defined seven postembryonic developmental stages for *A. ocellaris*, similar to the staging series previously produced for Zebrafish⁴⁶ and goldfish.⁶⁶ The method used to identify those different developmental stages may be modified for any other fish species as a tool to standardize sampling strategies and experimental procedures through the larval development.

4.1 | Shift in growth trajectory

All the quantitative criteria measured were correlated with both age and standard length, and as is the case for other teleost fish species, including Zebrafish (*D. rerio*) and tilapia (*Oreochromis mossambicus*), standard length is a better proxy than absolute age to describe developmental progression.^{49,67} In other species of Pomacentridae, studies have highlighted the high correlation between quantitative traits and the length of larval *A. frenatus* and *A. perideraion* (with a regression coefficients between 0.95 and 0.99),^{30,65} which has also been observed in *A. ocellaris* in this study. In general, allometric growth is common among clownfishes and all Pomacentridae,⁵⁵ but we can point out some interspecific differences. In *A. ocellaris*, we observed two distinct growth phases, the first one being relatively slow in our rearing condition (0.06 mm/day at 25°C) compared to the second growth phase: (SL = 0.2 mm/day). This second phase is characterized by a faster mean growth rate than in *A. frenatus* and *A. perideraion* (respectively, 0.4 mm/day and 0.3 mm/day between 27°C and

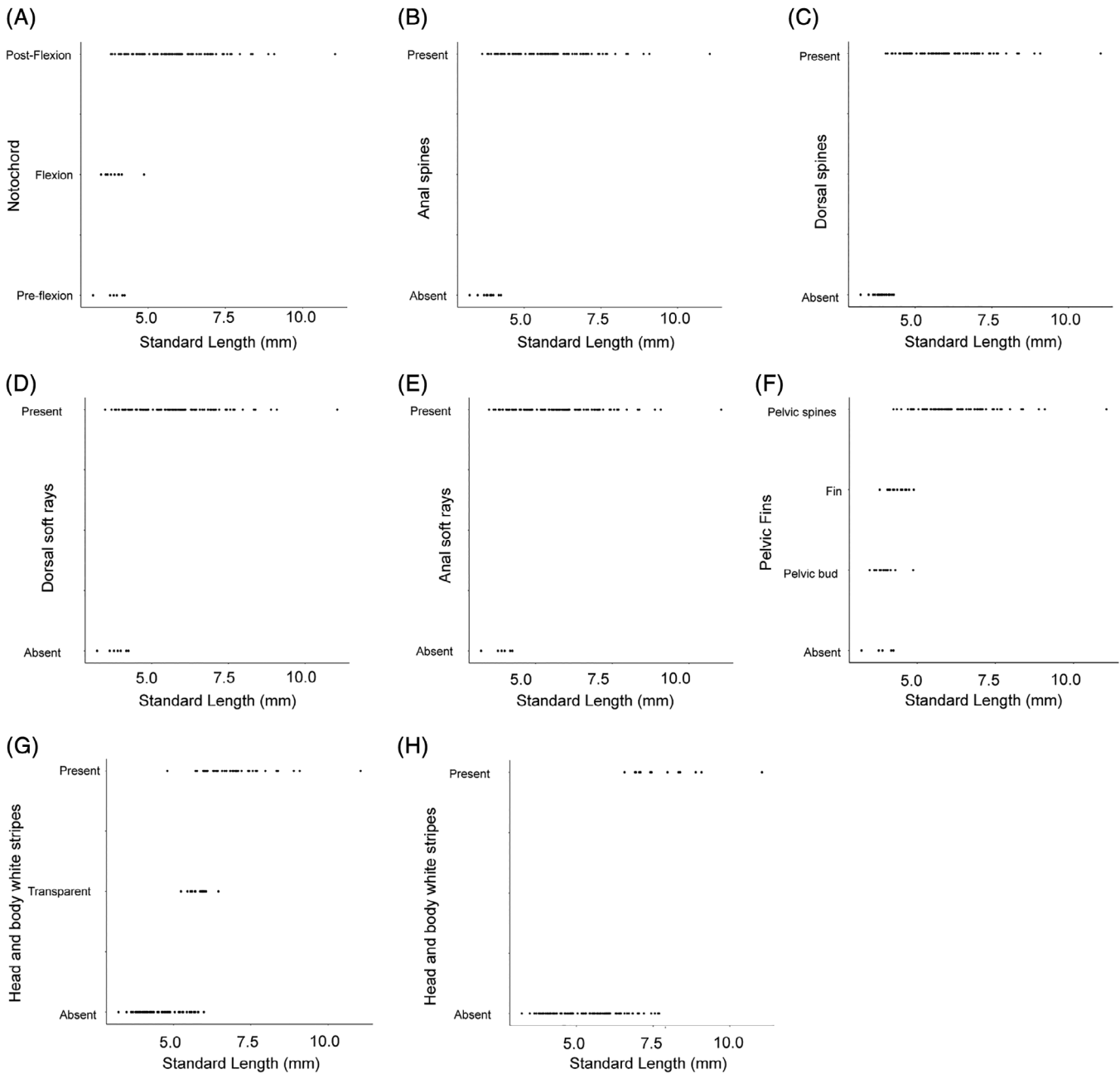


FIGURE 20 Variability in developmental progress. A–H: Graphics showing the developmental progress of each qualitative criteria according to the standard length. A: Notochord flexion; B: anal spines presence; C: dorsal spines presence; D: dorsal soft ray presence; E: anal soft rays presence; F: pelvic fin development; G: head and body white stripes; H: head white stripes

28°C). However, *A. frenatus* and *A. perideraion* show only a single growth trajectory and do not change slope. It is important to note that the rearing temperature and the size at 1 dph may explain those differences, as *A. ocellaris* measure 3.8 mm (± 0.5) and *A. frenatus* and *A. perideraion* measure 4.6 mm (± 0.1) and 4.4 mm (± 0.2), respectively, at hatching.^{41,65} In other more distant species of Pomacentridae, such as *Pomacentrus amboinensis*, there is also an increase of the growth rates during the second growth phase at 7 dph. In *P. amboinensis*, as in *A. ocellaris*, this acceleration occurred when larvae were in postflexion.⁵⁵ The existence of two

growth phases, referred to as a shift in growth trajectory, has also been observed in other fish species, such as several Blenniidae, *O. mossambicus*, *Paralichthys californicus*, and *Epinephelus marginatus*.^{63,67-69} This shift in growth trajectory can be linked with the onset of metamorphosis, which is a major phase in fish larval development as it allows the transition between the larval (generally pelagic in marine species) and the juvenile (generally demersal) stages.^{56,69}

Even if SL is a better proxy to follow the larval development of *A. ocellaris*, there is likely some variability in developmental progress even within a given SL category; this has been

observed in Zebrafish.^{46,49} Indeed, Parichy et al⁴⁶ observed that for a given size, larvae may not be at the same developmental stage. This is true also in *A. ocellaris* since we observed that individuals measuring 3.8 mm can be in flexion or in post-flexion, have anal spines or not, and have a pelvic bud or not (Figure 20). The establishment of a developmental table based on qualitative criteria is an efficient way to overcome this heterogeneity and develop the clownfish as a model system for developmental biology.

4.2 | Developmental stages

Based on the work done on the goldfish and the Zebrafish, we selected seven qualitative criteria easily visible under a brightfield stereomicroscope or a binocular loupe: the flexion of the notochord, the appearance of the anal and dorsal soft rays and spines, the development of the pelvic fin, and the appearance of the three white stripes.^{46,66} As traits are highly variable between species, the criteria used in our studies were not the same as those used for goldfish or Zebrafish. For example, Parichy et al⁴⁶ used the flexion angle as developmental criteria, but, as in goldfish, this criterion seems not obvious to apply for clownfish, as in our conditions it is difficult to measure in late-stage larvae due to their pigmentation, which covers the notochord. To determine flexion of the notochord, we used the position of the hypural bones, as it is commonly used in descriptions of larval fish development.^{70,71} As in many fish species, hypural bones are the first skeletal structures to appear in the caudal fin.⁷⁰⁻⁷³ For similar reasons, we did not use the swim bladder as a criterion because it is hidden by melanophores through all the larval development of *A. ocellaris*. This has also been noted in *E. marginatus* and *A. perideraion* larvae.^{41,69}

4.3 | Dissociation between morphological and pigmentation changes

Interestingly, as in *A. perideraion*, we observed a decoupling between the morphological and pigmentation changes.⁴¹ Indeed, most of the morphological changes of *A. ocellaris* appear during stages 1 to 4, and pigmentation changes start at stage 5 (with the progression of orange xanthophores and the appearance of white stripes). This decoupling may indicate the timing of the metamorphosis of *A. ocellaris*, which would be mainly characterized by pigmentation changes and not by drastic morphological changes, as it has been observed in grouper, flatfish, or surgeonfish.^{8,11,74} In those species, it is known that thyroid hormones are controlling metamorphosis as in amphibians,⁷⁵ and it has been shown that these hormones markedly affect overall growth and development rates, as well as individual traits including pigmentation and scales,⁷⁶ feeding kinematics,⁷⁷ and morphometrics and the lateral line.⁷⁸ It is similarly likely that thyroid hormones control the morphological

and pigmentation changes that occur during *A. ocellaris* metamorphosis.

5 | CONCLUSION

In this study, we provided the first postembryonic developmental table for a coral reef fish: the clownfish *A. ocellaris*. This table is characterized by seven larval stages. It is our hope that this staging tool will facilitate work with *A. ocellaris* as a model species, which can be used to better understand how coral reef fish larval development is regulated and how it may be impacted by environmental perturbations.

6 | EXPERIMENTAL PROCEDURES

6.1 | Breeding care

A. ocellaris larvae were obtained from three different clutches laid by a 10-year-old breeding pair. The breeding pair was held in a 200-L tank of artificial sea water at a temperature of 25°C, 35 g/L salinity, and a 12:12 light:dark photoperiod. Adult fish were fed twice daily with live food including shrimp, mussels, and sardines. Egg clutches were laid on a terra-cotta pot in the breeding tank. Eight days after fertilization, larvae were transferred to a 30-L rearing tank filled with water from the parental aquarium. Temperature and salinity were maintained identical to parental aquarium. Larvae were fed with rotifers *Brachionus plicatilis* (enriched with *Nannochloropsis* sp.) at 10 rotifers/ml⁻¹ three times a day during the first six days. *Artemia* nauplii were added at 6 dph, and the ratio of *Artemia*/rotifers was increased until larvae were fed exclusively with *Artemia* at 10 dph. At 15 dph, metamorphosed juveniles were fed with *Artemia* and pellets (Ocean Nutrition). Daily water changes (20% of total volume) were performed from day two onward to eliminate dead larvae and avoid nitrite and nitrate buildup.

6.2 | Description of larval development and stage identification

To follow the developmental changes occurring during larval development, we chose to identify both quantitative (eg, standard length, body depth, etc.) and qualitative (eg, appearance of fin rays, notochord flexion, pigmentation, etc.) (Table 1; Figure 4B) traits. Pictures of at least three larvae (euthanized in a 200-mg/L⁻¹ MS222 solution; Sigma-Aldrich) were taken daily from 1 dph to 21 dph, and at 30 dph under a stereomicroscope with brightfield-transmitted and incident illumination (ZEISS V20 discovery-Plan S objective 1.0 × equipped with an AxioCam 105 camera). Larvae were placed in a drop of filtered sea water on a Petri dish under the stereomicroscope. For each individual, a picture of the whole larva was taken at a 10×

magnification to assess the eight selected quantitative traits. Measurements were performed using ImageJ software (V1.51k).⁷⁹ All quantitative variables were analyzed using R,⁸⁰ and we used SD to quantify the amount of variation within our sampling. Binary and multinomial logistic regression models were applied with the package “rms” on R to determine the best variable between age and SL explaining the qualitative criteria.⁸¹ To define the developmental stages, individuals were categorized according to the chronological appearance of the different qualitative criteria.

6.3 | Scanning electron microscopy

The protocol used to prepare the samples is adapted from Arvedlund et al.²³ Samples were collected during the larval development and fixed in a solution of glutaraldehyde 2.5% in sodium cacodylate 0.1 M and 0.1 M sucrose buffer. Samples were then washed in sodium cacodylate 0.1 M and 10% sucrose buffer, then post-fixed one hour at 4° in a 1% osmium solution before dehydration. Final steps of the dehydration were done in an HMDS (hexamethyldisilane) solution. Samples were dried overnight prior to metallization with gold palladium before observation with a Hitachi S800.

6.4 | Phylogenetic tree

In order to illustrate the phyletic position of *A. ocellaris* among other fish models, we retrieved phylogenetic hypothesis via the Fish Tree of Life website by using the function `fishree_phylogeny` from the R-package `fishree`.⁸²

6.5 | Ethics approval

These experiments were approved by the C2EA-36 Ethics Committee for Animal Experiment Languedoc-Roussillon (CEEA-LR), number A6601601. We have an approval number (A6601601) of premises for animal testing issued by the Regional Directorate of Food, Agriculture and Forestry of Occitania, and the Departmental Directorate of Protection of Populations of the Pyrenees Orientales. The animals were raised in our lab from breeding stock. Experimental protocols were based on the regulations in force in France (Articles R214-87 to R214-137 of the Rural Code), updated by Decree 2013-118 and by five decrees dated February 1, 2013, and published February 7, 2013, pursuant to Directive 2010/63/EU. This regulation is under the responsibility of the Ministry of Agriculture.

ACKNOWLEDGMENTS

We thank the aquariology service of the marine station of Banyuls-sur-Mer, who provided the larvae used in this study. We also thank the Biopic platform of the marine

station of Banyuls-sur-Mer for its help on the morphological observations. We thank the technological center of the microstructures where the scanning electron microscopic observations were made. We thank Yves Desdevises and Laurence Besseau (BIOM UMR 7232) for their help with the statistical analyses and the writing of the manuscript. We thank Sarah Mc Menamin for critical reading of the manuscript and many useful suggestions. Our rearing structure of clownfish has been supported by the CNRS (interdisciplinarity actions) and EMBRC France.

CONFLICT OF INTEREST

The authors declare that they have no competing interests.

ORCID

Natacha Roux  <https://orcid.org/0000-0002-1883-7728>

Vincent Laudet  <https://orcid.org/0000-0003-4022-4175>

REFERENCES

1. Majumdar SD, Hazra S, Giri S, et al. Threats to coral reef diversity of Andaman Islands, India: A review. *Reg Stud Mar Sci.* 2018;24: 237-250.
2. Roberts CM. Marine Biodiversity Hotspots and Conservation Priorities for Tropical Reefs. *Science.* 2002;295:1280-1284.
3. UNEP-WCMC. *In the Front line: Shoreline Protection and Other Ecosystem Services from Mangroves and Coral Reefs.* Cambridge, UK: UNEP-WCMC; 2006.
4. Principe P, Bradley P, Yee S, Fisher W, Johnson E, Allen P, Campbell D. U.S. Environmental Protection Agency, Office of Research and Development. Quantifying coral reef ecosystem services. <http://www.epa.gov/ged/quantify.pdf>. Published 2012. Accessed May 10, 2019.
5. Cesar H, Burke L, Pet-Soede L. *The economics of worldwide coral reef degradation.* Anherm, The Netherlands: Cesar Environmental Economics Consulting (CEEC); 2003.
6. Leis JM, McCormick MI. The Biology, Behavior, and Ecology of the Pelagic, Larval Stage of Coral Reef Fishes. *Coral Reef Fishes Dyn Divers Complex Ecosystem.* San Diego, CA: Academic Press; 2002:171-199.
7. Lecchini D, Galzin R. Synthèse sur l'influence des processus pélagiques et benthiques, biotiques et abiotiques, stochastiques et déterministes, sur la dynamique de l'autorecrutement des poissons coralliens. *Cybiuim.* 2003;27:167-184.
8. Holzer G, Besson M, Lambert A, et al. Fish larval recruitment to reefs is a thyroid hormone-mediated metamorphosis sensitive to the pesticide chlorpyrifos. *Elife.* 2017;6. pii:e27595.
9. Leis JM. Ontogeny of behaviour in larvae of marine demersal fishes. *Ichthyol Res.* 2010;57:325-342.
10. Barth P, Berenshtein I, Besson M, et al. From the ocean to a reef habitat: how do the larvae of coral reef fishes find their way home. *Vie at Milieu.* 2015;65:91-100.
11. McMenamin SK, Parichy DM. Metamorphosis in Teleosts. *Curr Top Dev Biol.* 2013;103:127-165.

12. Lecchini D, Dixson DL, Lecellier G, et al. Habitat selection by marine larvae in changing chemical environments. *Mar Pollut Bull.* 2017;114:210-217.
13. Bertucci F, Jacob H, Mignucci A, et al. Decreased retention of olfactory predator recognition in juvenile surgeon fish exposed to pesticide. *Chemosphere.* 2018;208:469-475.
14. Johansen JL, Allan BJM, Rummer JL, Esbaugh AJ. Oil exposure disrupts early life-history stages of coral reef fishes via behavioural impairments. *Nat Ecol Evol.* 2017;1:1146-1152.
15. Munday PL, Dixson DL, Donelson JM, et al. Ocean acidification impairs olfactory discrimination and homing ability of a marine fish. *Proc Natl Acad Sci.* 2009;106:1848-1852.
16. Dixson DL, Munday PL, Jones GP. Ocean acidification disrupts the innate ability of fish to detect predator olfactory cues. *Ecol Lett.* 2010;13:68-75.
17. O'Connor NJ, Van BT. Adult fiddler crabs *Uca pugnax* (Smith) enhance sediment-associated cues for molting of conspecific megalopae. *J Exp Mar Biol Ecol.* 2006;335:123-130.
18. Holles S, Simpson S, Radford A, Berten L, Lecchini D. Boat noise disrupts orientation behaviour in a coral reef fish. *Mar Ecol Prog Ser.* 2013;485:295-300.
19. Munday PL, Jones GP, Pratchett MS, Williams AJ. Climate change and the future for coral reef fishes. *Fish Fish.* 2008;9:261-285.
20. Elliott JK, Elliot JM, Mariscal RN. Host selection, location, and association behaviors of anemonefishes in field settlement experiments. *Mar Biol.* 1995;122:377-389.
21. Arvedlund M, McCormick MI, Fautin DG, Bildsoe M. Host recognition and possible imprinting in the anemonefish *Amphiprion melanopus* (Pisces: Pomacentridae). *Mar Ecol Prog Ser.* 1999; 188:207-218.
22. Arvedlund M, Larsen K, Winsor H. The embryonic development of the olfactory system in *Amphiprion melanopus* (Perciformes: Pomacentridae) related to the host imprinting hypothesis. *J Mar Biol Assoc UK.* 2000;80:1103-1109.
23. Arvedlund M, Munday PL, Takemura A. The morphology and ultrastructure of the peripheral olfactory organ in newly metamorphosed coral-dwelling gobies, *Paragobiodon xanthosomus* Bleeker (Gobiidae, Teleostei). *Tissue Cell.* 2007;39:335-342.
24. Scott A, Dixson DL. Reef fishes can recognize bleached habitat during settlement: sea anemone bleaching alters anemonefish host selection. *Proc R Soc B Biol Sci.* 2016;283:20152694.
25. Chivers DP, Dixson DL, White JR, McCormick MI, Ferrari MCO. Degradation of chemical alarm cues and assessment of risk throughout the day. *Ecol Evol.* 2013;3:3925-3934.
26. Liew HJ, Ambak MA, Abol-Munafi AB. Embryonic development of clownfish *Amphiprion ocellaris* under laboratory conditions. *J Sustain Manag.* 2006;1:64-73.
27. Madhu K, Madhu R, Krishnan L, Sasidharan CS, Venugopal KM. Spawning and larval rearing of *Amphiprion ocellaris* under captive condition. *Mar Fish Inf Serv Tech Ext Ser.* 2006;188:1-5.
28. Yasir I, Qin JG. Embryology and early ontogeny of an anemonefish *Amphiprion ocellaris*. *J Mar Biol Assoc UK.* 2007;87:1025-1033.
29. Ghosh J, Wilson RW, Kudoh T. Normal development of the tomato clownfish *Amphiprion frenatus*: live imaging and in situ hybridization analyses of mesodermal and neurectodermal development. *J Fish Biol.* 2009;75:2287-2298.
30. Salis P, Lorin T, Lewis V, et al. Developmental and comparative transcriptomic identification of iridophore contribution to white barring in clownfish. *Pigment Cell Melanoma Res.* 2019;32:391-402.
31. Ollerton J, McCollin D, Fautin DG, Allen GR. Finding NEMO: nestedness engendered by mutualistic organization in anemonefish and their hosts. *Proc R Soc B Biol Sci.* 2007;274:591-598.
32. Colleye O, Iwata E, Parmentier E. Clownfishes. In: Bruno F, Parmentier E, eds. *Biology of Damselfishes*. Boca Raton, FL: CRC Press; 2016:246-266.
33. Eschmeyer WN, Fricke R, Van der Laan R, eds. California Academy of Sciences. Catalog of fishes: species. <http://researcharchive.calacademy.org/research/ichthyology/catalog/fishcatmain.asp>. Updated May 6, 2019. Accessed May 10, 2019.
34. Davesne D, Gallut C, Barriel V, Janvier P, Lecointre G, Otero O. The phylogenetic intrarelationships of spiny-rayed fishes (Acanthomorpha, Teleostei, Actinopterygii): fossil taxa increase the congruence of morphology with molecular data. *Front Ecol Evol.* 2016;4:129.
35. Betancur RR, Wiley EO, Arratia G, et al. Phylogenetic classification of bony fishes. *BMC Evol.* 2017;17:162.
36. Hughes LC, Ortí G, Huang Y, et al. Comprehensive phylogeny of ray-finned fishes (Actinopterygii) based on transcriptomic and genomic data. *Proc Natl Acad Sci.* 2018;115:6249-6254.
37. Cooper WJ, Carter CB, Conith AJ, Rice AN, Westneat MW. The evolution of jaw protrusion mechanics is tightly coupled to benthic-pelagic divergence in damselfishes (Pomacentridae). *J Exp Biol.* 2017;220:652-666.
38. Olivier D, Frédéric B, Spanopoulos-Zarco M, Balart EF, Parmentier E. The cerato-mandibular ligament: a key functional trait for grazing in damselfishes (Pomacentridae). *Front Zool.* 2014;11:63.
39. Parmentier E, Colleye O, Fine ML, Frédéric B, Vandewalle P, Herrel A. Sound production in the clownfish *Amphiprion clarkii*. *Science.* 2007;316:1006-1006.
40. Parmentier E, Kéver L, Casadevall M, Lecchini D. Diversity and complexity in the acoustic behaviour of *Dacyllus flavicaudus* (Pomacentridae). *Mar Biol.* 2010;157:2317-2327.
41. Salis P, Roux N, Lecchini D, Laudet V. The post-embryonic development of *Amphiprion perideraion* reveals a decoupling between morphological and pigmentation changes. *Cybium.* 2018;42:309-312.
42. Salis P, Roux N, Soulat O, Lecchini D, Laudet V, Frédéric B. Ontogenetic and phylogenetic simplification during white stripe evolution in clownfishes. *BMC Biol.* 2018;16:90.
43. Marcionetti A, Rossier V, Roux N, Salis P, Laudet V, Salamin N. Insights into the genomics of clownfish adaptive radiation: Genetic basis of the mutualism with sea anemones. *Genome Biol Evol.* 2019; 11:869-882.
44. Hopwood N. A history of normal plates, tables and stages in vertebrate embryology. *Int J Dev Biol.* 2007;51(1):1-26.
45. Kimmel CB, Ballard WW, Kimmel SR, Ullmann B, Schilling TF. Stages of Embryonic Development of the Zebrafish. *Dev Dyn.* 1995;203:253-310.
46. Parichy DM, Elizondo MR, Mills MG, Gordon TN, Engeszer RE. Normal table of postembryonic zebrafish development: Staging by externally visible anatomy of the living fish. *Dev Dyn.* 2009;238: 2975-3015.
47. Nieuwkoop PD, Faber J. *Normal table of Xenopus laevis (Daudin): a systematic and chronological survey of the development from the fertilized egg till the end of metamorphosis*. 2nd ed. Amsterdam, The Netherlands: North-Holland Publishing Company; 1967.
48. Ribeiro FF, Forsythe S, Qin JG. Dynamics of intracohort cannibalism and size heterogeneity in juvenile barramundi (*Lates calcarifer*) at different stocking densities and feeding frequencies. *Aquaculture.* 2015;444:55-61.

49. McMenamin SK, Chandless MN, Parichy DM. Working with zebrafish at postembryonic stages. *Methods Cell Biol.* 2016;134:587-607.
50. Villamizar N, Blanco-Vives B, Migaud H, Davie A, Carboni S, Sánchez-Vázquez FJ. Effects of light during early larval development of some aquacultured teleosts: A review. *Aquaculture.* 2011;315:86-94.
51. Mojjada SK, Dash B, Pattnaik P, Anbarasu M, Imelda J. Effect of stocking density on growth and survival of hatchery reared fry of Asian seabass, *Lates calcarifer* (Bloch) under captive conditions. *Indian J Fish.* 2013;60:71-75.
52. McLeod IM, Jones RE, Jones GP, Takahashi M, McCormick MI. Interannual variation in the larval development of a coral reef fish in response to temperature and associated environmental factors. *Mar Biol.* 2015;162:2379-2389.
53. Fautin DG, Allen GR. Anemonefishes and their host sea anemones: a guide for aquarists and divers. Perth, WA: Western Australian Museum; 1997.
54. Cucchi P, Sucré E, Santos R, Leclère J, Charmantier G, Castille R. Embryonic development of the sea bass *Dicentrarchus labrax*. *Helgol Mar Res.* 2012;66:199-209.
55. Kavanagh KD, Frederich B. Ontogeny and Early Life Stages of Damselfishes. In: Frederich B, Parmentier E, eds. *Biology of Damselfishes*. Vol 1. Boca Raton, FL: CRC Press; 2016.
56. McCormick MI, Makey L, Dufour V. Comparative study of metamorphosis in tropical reef fishes. *Mar Biol.* 2002;141:841-853.
57. Laudet V. The Origins and Evolution of Vertebrate Metamorphosis. *Curr Biol.* 2011;21:R726-R737.
58. Victor BC, Wellington GM. Endemism and the pelagic larval duration of reef fishes in the eastern Pacific Ocean. *Mar Ecol Prog Ser.* 2000;205:241-248.
59. Leis JM, Siebeck U, Dixon DL. How nemo finds home: The neuroecology of dispersal and of population connectivity in larvae of marine fishes. *Integr Comp Biol.* 2011;51:826-843.
60. Dixon DL, Munday PL, Pratchett M, Jones GP. Ontogenetic changes in responses to settlement cues by Anemonefish. *Coral Reefs.* 2011;30:903-910.
61. Madhu R, Madhu K, Rethesh T. Life history pathways in false clown Amphiprion ocellaris Cuvier, 1830: A journey from egg to adult under captive condition. *J Mar Biol Assoc India.* 2012;54:77-90.
62. Buston P. Social hierarchies: size and growth modification in clownfish. *Nature.* 2003;424:145-146.
63. Gisbert E. Morphological development and allometric growth patterns in hatchery-reared California halibut larvae. *J Fish Biol.* 2002;61:1217-1229.
64. Murphy BF, Leis JM, Kavanagh KD. Larval development of the Ambon damselfish *Pomacentrus amboinensis*, with a summary of pomacentrid development. *J Fish Biol.* 2007;71:569-584.
65. Putra DF, Abol-Munafi AB, Muchlisin ZA, Chen J-C. Preliminary studies on morphology and digestive tract development of tomato clownfish, *Amphiprion frenatus* under captive condition. *Aquac Aquar Conserv Legis.* 2012;5:29-35.
66. Li I-J, Chang C-J, Liu S-C, Abe G, Ota KG. Postembryonic staging of wild-type goldfish, with brief reference to skeletal systems: Goldfish Postembryonic Staging. *Dev Dyn.* 2015;244:1485-1518.
67. Campinho MA, Moutou KA, Power DM. Temperature sensitivity of skeletal ontogeny in *Oreochromis mossambicus*. *J Fish Biol.* 2004;65:1003-1025.
68. Ditty JG, Shaw RF, Fuiman LA. Larval development of five species of blenny (Teleostei: Blenniidae) from the western central North Atlantic, with a synopsis of blennioid family characters. *J Fish Biol.* 2005;66:1261-1284.
69. Cunha ME, Ré P, Quental-Ferreira H, Gavaia PJ, Pousão-Ferreira P. Larval and juvenile development of dusky grouper *Epinephelus marginatus* reared in mesocosms: larval development of *Epinephelus marginatus*. *J Fish Biol.* 2013;83:448-465.
70. Laggis A, Sfakianakis DG, Divanach P, Kentouri M. Ontogeny of the body skeleton in *Seriola dumerili* (Risso, 1810). *Ital J Zool.* 2010;77:303-315.
71. Woltering JM, Holzem M, Schneider RF, Nanos V, Meyer A. The skeletal ontogeny of *Astatotilapia burtoni*—a direct-developing model system for the evolution and development of the teleost body plan. *BMC Dev Biol.* 2018;18:8.
72. Fujita K. Ontogeny of the caudal skeleton in the clariid catfish *Clarias batrachus*. *Jpn J Ichthyol.* 1992;38:430-432.
73. Bensimon-Brito A, Cancela ML, Huysseune A, Witten PE. Vestiges, rudiments and fusion events: the zebrafish caudal fin endoskeleton in an evo-devo perspective: Vertebral fusion in the zebrafish caudal skeleton. *Evol Dev.* 2012;14:116-127.
74. de Jesus EG, Toledo JD, Simpás MS. Thyroid hormones promote early metamorphosis in grouper (*Epinephelus coioides*) larvae. *Gen Comp Endocrinol.* 1998;112:10-16.
75. Grimaldi A, Buisine N, Miller T, Shi Y-B, Sachs LM. Mechanisms of thyroid hormone receptor action during development: Lessons from amphibian studies. *Biochim Biophys Acta.* 2013;1830:3882-3892.
76. McMenamin SK, Bain EJ, McCann AE, et al. Thyroid hormone-dependent adult pigment cell lineage and pattern in zebrafish. *Science.* 2014;345:1358-1361.
77. McMenamin S, Carter C, Cooper WJ. Thyroid Hormone Stimulates the Onset of Adult Feeding Kinematics in Zebrafish. *Zebrafish.* 2017;14:517-525.
78. Hu Y, Mauri A, Donahue J, Singh R, Acosta B, McMenamin SK. Thyroid hormone coordinates developmental trajectories but does not underlie developmental truncation in Danionins. *bioRxiv.* 2019;562074.
79. Schneider CA, Rasband WS, Eliceiri KW. NIH Image to ImageJ: 25 years of Image Analysis. *Nat Methods.* 2012;9:671-675.
80. R Development Core Team. R: A language and environment for statistical computing. R Foundation for Statistical Computing. Vienna, Austria. <http://www.R-project.org/>. May 10, 2019.
81. Harrell FE Jr. 2019. Package “rms.” <https://cran.r-project.org/web/packages/rms/rms.pdf>. Published April 22, 2019. Accessed May 20, 2019.
82. Chang J, Rabosky DL, Smith SA, Alfaro ME. An r package and online resource for macroevolutionary studies using the ray-finned fish tree of life. *Methods Ecol Evol.* 2019. <https://doi.org/10.1111/2041-210X.13182>.

How to cite this article: Roux N, Salis P, Lambert A, et al. Staging and normal table of postembryonic development of the clownfish (*Amphiprion ocellaris*). *Developmental Dynamics.* 2019;248:545–568. <https://doi.org/10.1002/dvdy.46>